

# A Peptide Nucleic Acid–Aminosugar Conjugate Targeting Transactivation Response Element of HIV-1 RNA Genome Shows a High Bioavailability in Human Cells and Strongly Inhibits Tat-Mediated Transactivation of HIV-1 Transcription

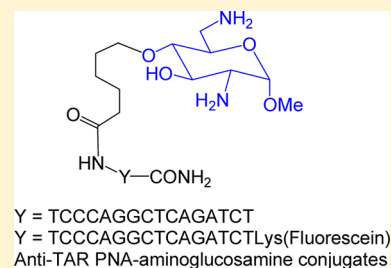
Indrajit Das,<sup>†</sup> Jérôme Désiré,<sup>†,§</sup> Dinesh Manvar,<sup>‡</sup> Isabelle Baussanne,<sup>†</sup> Virendra N. Pandey,<sup>\*,‡</sup> and Jean-Luc Décout<sup>\*,†</sup>

<sup>†</sup>Université de Grenoble I/CNRS, UMR 5063, Département de Pharmacochimie Moléculaire, ICMG FR 2607, 470 rue de la Chimie BP 53, F-38041 Grenoble, France

<sup>‡</sup>Center for the Study of Emerging and Re-emerging Pathogens, UMDNJ—New Jersey Medical School, Department of Biochemistry and Molecular Biology, 185 South Orange Avenue, Newark, New Jersey 07103, United States

## Supporting Information

**ABSTRACT:** The 6-aminoglucosamine ring of the aminoglycoside antibiotic neomycin B (ring II) was conjugated to a 16-mer peptide nucleic acid (PNA) targeting HIV-1 TAR RNA. For this purpose, we prepared the aminoglucosamine monomer **15** and attached it to the protected PNA prior to its cleavage from the solid support. We found that the resulting PNA–aminoglucosamine conjugate is stable under acidic conditions, efficiently taken up by the human cells and fairly distributed in both cytosol and nucleus without endosomal entrapment because cotreatment with endosome-disrupting agent had no effect on its cellular distribution. The conjugate displayed very high target specificity in vitro and strongly inhibited Tat mediated transactivation of HIV-1 LTR transcription in a cell culture system. The unique properties of this new class of PNA conjugate suggest it to be a potential candidate for therapeutic application.



## INTRODUCTION

Aminoglycosides such as neomycin B **1** (Figure 1) are highly potent and broad-spectrum pseudo-oligosaccharidic antibiotics which act by binding to 16S rRNA, causing mRNA decoding errors, mRNA and tRNA translocation blockage, ribosome recycling inhibition, and in fine protein synthesis alteration.<sup>1–5</sup> The strong affinities of aminoglycosides for other RNA targets such as several ribozymes<sup>6–16</sup> and important RNA motifs of HIV, the transactivation response element (TAR), the rev responsive element (RRE), and the dimerization initiation site (DIS),<sup>17–20</sup> led to intensive works for their modifications in the search for RNA-targeting drugs.<sup>21–25</sup> Amphiphilic aminoglycosides have been also reported as antimicrobial agents<sup>26–34</sup> targeting bacterial rRNA and/or membranes<sup>33,34</sup> and as efficient gene<sup>35,36</sup> and siRNA<sup>37</sup> delivery vectors.

In the antisense approach for RNA targeting,<sup>38,39</sup> the conjugation of aminoglycoside to oligonucleotides or peptide (polyamide) nucleic acids (PNA) is attractive because the strong binding of the covalently attached aminoglycoside may enhance hybridization and direct the drug design to shorter oligonucleotide sequences. Aminoglycosides are able to stabilize DNA- and RNA-triplexes and DNA–RNA hybrid triplexes and hybrid duplexes.<sup>40–42</sup> Improvements in the cellular uptake also may be provided because neomycin has been shown to assist the lipid-mediated delivery of oligonucleotides.<sup>43</sup> Because of the presence of protonated and

unprotonated amino groups in the neamine core, an acido-basic catalysis of hydrolysis of the target RNA could be expected.<sup>44</sup> A number of aminoglycoside antibiotics, and in particular neomycin B, were demonstrated to promote strand cleavage of RNA oligonucleotides (minimized HIV-1 TAR element and prokaryotic ribosomal A-site) by binding and causing sufficient distortion to the RNA backbone to render it more susceptible to intramolecular transphosphorylation.<sup>45,46</sup> Regarding the conjugation of aminoglycosides to oligo-2'-deoxyribonucleotides (ODN), neomycin has been covalently attached to the 5'-end of an ODN complementary to a seven-bases long  $\alpha$ -sarcin loop RNA sequence, and its ability to enhance duplex formation has been studied.<sup>47</sup> A set of neamine- and ribostamycin-2'-O-methyl oligoribonucleotide conjugates has been prepared in order to study their nuclease activity.<sup>48</sup> Neamine and paromamine–ODN conjugates were also synthesized using click chemistry, and DNA duplex stabilization was observed with a paromamine conjugate.<sup>49,50</sup> More recently, aminoglycoside (neomycin, ribostamycin, and methyl neobiosamine) conjugated to the 3'-end of 2'-O-methyl oligoribonucleotides were synthesized to target a <sup>19</sup>F labeled HIV-1 TAR RNA model which allows monitoring of the invasion by <sup>19</sup>F NMR spectrometry.<sup>51</sup> A remarkably enhanced invasion,

Received: December 6, 2011

Published: June 14, 2012

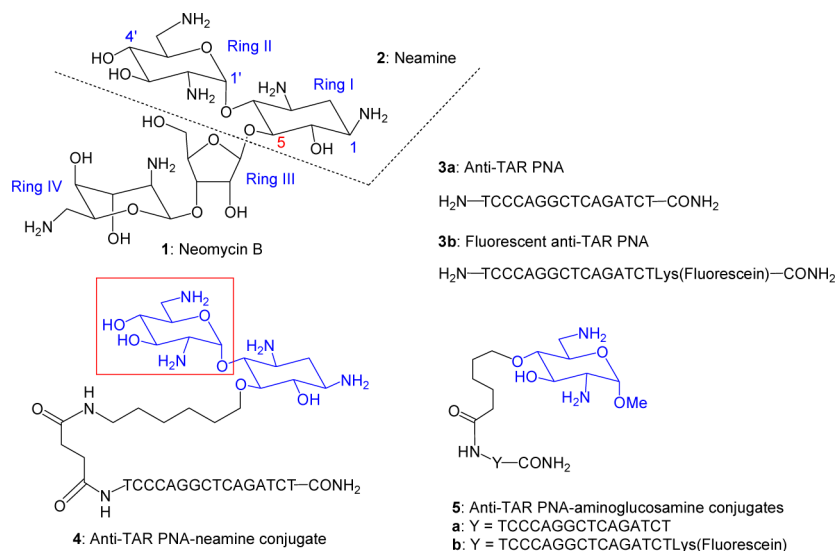


**Figure 1.** Structure of neomycin B, neamine, the anti-TAR PNA, and the corresponding neamine and 6-aminoglycosamine conjugates **4**, **5a**, and **5b**.

compared to that resulting from the corresponding unmodified 2'-O-methyl oligoribonucleotide was observed with the neomycin conjugate. The conjugation of neamine to dinucleotides has been reported to remarkably decrease affinity to HIV-1 TAR RNA due to electrostatic repulsion between the phosphates, whereas conjugates of the corresponding PNA show about 2-fold binding affinities compared to that of neamine.<sup>52</sup> In the antisense approach with ODN conjugates, the strong binding of aminoglycosides to nucleic acids also probably leads to intramolecular and intermolecular charge-charge interaction between the protonated aminoglycoside core and the phosphodiester backbone of the ODN that can disturb the binding to the RNA target.

Peptide nucleic acids (PNAs) are a class of antisense DNA analogues first synthesized by Nielsen and colleagues in 1991.<sup>53</sup> The PNA molecules, devoid of sugar phosphate backbone and charges under physiological conditions, have been shown to display high affinity for complementary sequences on RNA and DNA both in single- and double-stranded forms.<sup>54–56</sup> PNA are highly stable and remained uncleaved when incubated with blood or cell lysate from human and bacterial cells.<sup>57</sup> Initial expectations held that PNAs would quickly enter the field of antisense as genespecific, nontoxic, and nonimmunogenic agents. However, problems associated with solubility and poor cellular uptake of this class of compounds hampered developments in this direction.<sup>58</sup> The synthesis of modified PNAs or PNA conjugates presents a new means of improving their solubility and cellular uptake.<sup>58</sup>

A number of strategies have been used for improving the biodelivery of naked or modified forms of PNA in cell culture systems or in vivo.<sup>58–61</sup> The major advance in biodelivery of PNA was made by conjugating cell-transducing agents, including cell penetrating peptides (CPP). A number of reviews on CPP and their therapeutic application have been reported.<sup>62–65</sup> A triphenyl-phosphonium-tagged PNA targeted to HIV-1 TAR was found to be efficiently taken up by cells and to block HIV-1 production in cell culture.<sup>66</sup> The major drawback in the PNA biodelivery system based on cell penetrating peptides is the endosomal entrapment of PNA in the cytosol, which limits its target efficacy.<sup>67</sup>

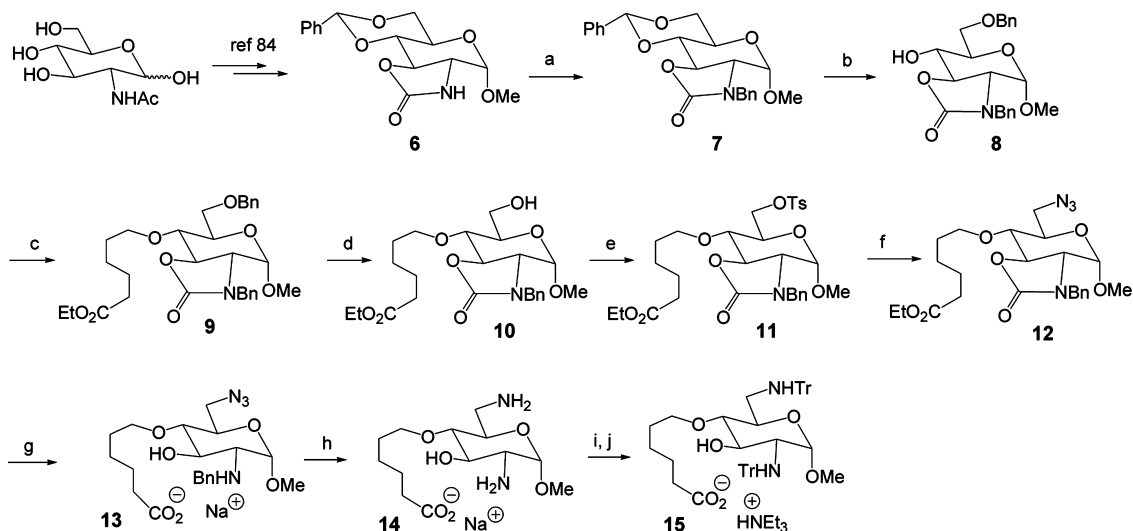
The most efficient cellular uptake of anti-HIV-1 PNA was noted with the use of cell-penetrating peptides (CPP) including

penetratin, transportan, and HIV-1 Tat-derived peptide as a vehicle to deliver anti-HIV-1 PNA into cells.<sup>68–70</sup> CPP vehicle specially the cationic CPP such as Tat and oligo-Arg carrying PNA cargoes has been shown to enter the cell via endosomal pathway.<sup>65,71</sup> Another major deterrent is that peptide carriers are unsuitable for oral biodelivery as they are prone to cleavage by gut proteases prior to their entry into the cells.

Methods for conjugation of PNA with aminoglycosides have also been reported.<sup>52,72–76</sup> In one unique study in the antisense approach, we have conjugated the neamine core **2** (Figure 1) corresponding to rings I and II of neomycin B **1** with the 16-mer PNA **3** targeting HIV-1 TAR RNA (anti-TAR PNA).<sup>75</sup> In the resulting conjugate **4** (Figure 1), the presence of the neamine core not only imparts greater solubility and enhanced cellular uptake of PNA, it also confers a unique metal-ion-independent target specific RNA cleavage property to the conjugate.<sup>75,76</sup> We also noted that unlike PNA–CPP conjugate, PNA–neamine is compatible with oral administration in mice and efficiently absorbed in the gut (unpublished data).

Probably, the presence of positive charges is necessary for the penetration of the conjugate **4** in human cells through interaction with the membrane phospholipids and disruption of the membrane integrity. To decrease the number of amine functions in conjugate **4** that may be protonated under physiological conditions and could be a source of toxicity and nonspecific interaction with the nontarget nucleic acid, our strategy was to conjugate the anti-TAR PNA sequence **3** to the small aminoglycosidic moiety 6-amino-6-deoxyglucosamine (neosamine) which corresponds to ring II of neamine (and neomycin).

N-Acetyl-D-glucosamine is the major constituent of the peptidoglycan polymer (murein) forming the bacterial cell wall and of the chitin polymer forming the exoskeleton of arthropods such as crustaceans (e.g., crabs). The chitosan polymers obtained by hydrolysis of chitin under basic conditions have been intensively used for preparing gene delivery vectors.<sup>77</sup> Aminosugars such as D-glucosamine have been also found to be able to weakly induce single-strand breakage in DNA that was increased in the presence of copper(II) ions.<sup>78–82</sup> In the search for antibacterial agents, 6-aminoglycosamine derivatives incorporating at the 1-position acyclic deoxystreptamine mimetics (ring I of neomycin B) have

Scheme 1. Synthesis of the Glucosamine Derivative 15 for Further Coupling to the Anti-TAR PNAs<sup>a</sup>

<sup>a</sup>Reagents and conditions: (a) BnBr, K<sub>2</sub>CO<sub>3</sub>, DMF, rt, 10 h, 84%; (b) Et<sub>3</sub>SiH, BF<sub>3</sub>·OEt<sub>2</sub>, CH<sub>2</sub>Cl<sub>2</sub>, 0 °C, 2 h, 81%; (c) 6-bromohexanoic acid ethyl ester, NaH, DMF, rt, 8 h, 92%; (d) H<sub>2</sub>, Pd/C (10%), EtOH, rt, 12 h, 98%; (e) TsCl, pyridine; rt, 10 h, 96%; (f) NaN<sub>3</sub>, DMF, 80 °C, 3 h, 91%; (g) 1 M NaOH, dioxane/H<sub>2</sub>O (4/1), 100 °C, 14 h, 74%; (h) HCO<sub>2</sub>NH<sub>4</sub>, Pd(OH)<sub>2</sub>/C (20%), MeOH/H<sub>2</sub>O (9/1), reflux, 1.5 h, 95%; (i) TrCl, DMF, Et<sub>3</sub>N, rt, 8 h, 68%; (j) 1 M NaOH/dioxane (1/1), 80 °C, 6 h, 85%.

been synthesized but none of them shows a high potency comparable to that of the natural aminoglycosides.<sup>83</sup> Here, we report on the synthesis of a 6-amino-6-deoxyglucosamine derivative and its conjugation to sequence specific PNA targeted to TAR element on HIV-1 genome. The resulting conjugate **5a** (Figure 1) is rapidly taken up by the cells and exhibits potent antiviral activity, thus suggesting a strong therapeutic potential for this class of molecules.

The prepared conjugate **5a** and the corresponding fluorescently tagged conjugate **5b** (Figure 1) were designed to carry only two positive charges under physiological conditions, whereas in the neamine conjugate **4**, four positive charges can be present. In **5a** and **5b**, the PNA and the linking chain were attached at the 4-oxygen atom of the neosamine moiety for a maximal distance of both protonated amine functions in regard to the possible crucial role of these functions for an efficient cellular uptake. A methyl group was introduced at the anomeric position of the neosamine moiety (1-methylneosamine) in order to stabilize the sugar ring and to minimize the steric hindrance at this position as well as the lipophilicity for clearly defining a charged polar head in the conjugate.

## SYNTHESIS

To link the 6-amino-D-glucosamine ring to the anti-TAR PNA sequence, inexpensive *N*-acetyl-D-glucosamine was used as a starting compound. The target glucosamine derivative **15** used for further coupling to the protected PNAs **3a** and **3b** was prepared in 14 steps (Scheme 1).

In comparison to the glucosamine moiety, a second amine function should be added at the 6-position and a methyl group at the 1-hemicetal function as well as a linking arm at the 4-position for attachment to the PNA. This arm should carry a terminal carboxylate group for coupling through an amide junction to the *N*-terminus of the protected anti-TAR PNAs.

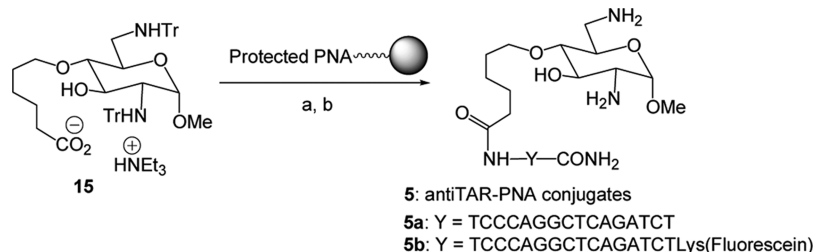
The first steps in the synthesis were performed according to the literature for obtaining the intermediate **6**<sup>84</sup> through (i) methylation of the anomeric hemiacetal function, (ii)

protection of the 4- and 6-hydroxyl functions by formation of the benzylidene derivative, and (iii) deacetylation to release the 2-amino function.

To protect the 3-hydroxyl function allowing the selective introduction of the linking chain from the free 4-hydroxyl group, the 2-amino function was protected in two steps as an oxazolidinone spanning the *N*-2 and *O*-3 atoms and bearing a benzyl group on the nitrogen atom.<sup>85</sup> Treatment of the resulting compound **7** with triethylsilane and BF<sub>3</sub> diethyl etherate allowed the selective deprotection of the 4-hydroxyl function to lead to **8**, which was alkylated with ethyl 6-bromohexanoate in order to introduce the protected linking arm. From the prepared ester **9**, the 6-*O*-benzyl group was removed by catalytic hydrogenation to release the 6-hydroxyl group.

A 6-azido group precursor of the additional 6-amino function was introduced through tosylation and then substitution of the tosyl group by reaction with sodium azide to lead to the derivative **12**. Treatment of **12** with aqueous NaOH opened the oxazolidinone ring, releasing the 3-hydroxyl function and the benzylated 2-amino function as well as a carboxylate function at the end of the linking chain in compound **13**. In the presence of palladium hydroxide and ammonium formate, it was possible to reduce concomitantly the 6-azido group and to debenzylate the 2-amino function of **13** to lead to the methyl-2,6-diaminoglucopyranoside **14** bearing the linking chain with a terminal carboxylate function.

To (i) link the methyl-2,6-diaminoglucopyranoside ring to the anti-TAR PNA sequence, (ii) deprotect the obtained conjugate under the conditions used to remove the benzhydryloxycarbonyl (Bhoc) groups employed in the PNA synthesis for protection of the amine functions of the bases, and (iii) cleave the conjugate from the solid support, trityl acid-labile protecting groups were introduced to protect the 2- and 6-amino functions of **14** and afforded compound **15** in two steps. It was not possible to introduce a 4-methoxybenzyl group to protect the remaining free 3-hydroxyl group of compound **13** probably due to a strong steric hindrance generated by the

Scheme 2. Synthesis of the PNA–Aminoglucosamine Conjugates **5a** and **5b**<sup>a</sup>

<sup>a</sup>Reagents and conditions: (a) EDC, HOBT, DMF, protected PNA **3a** or **3b**; (b) TFA/anisole (1/1), rt, 2 h.

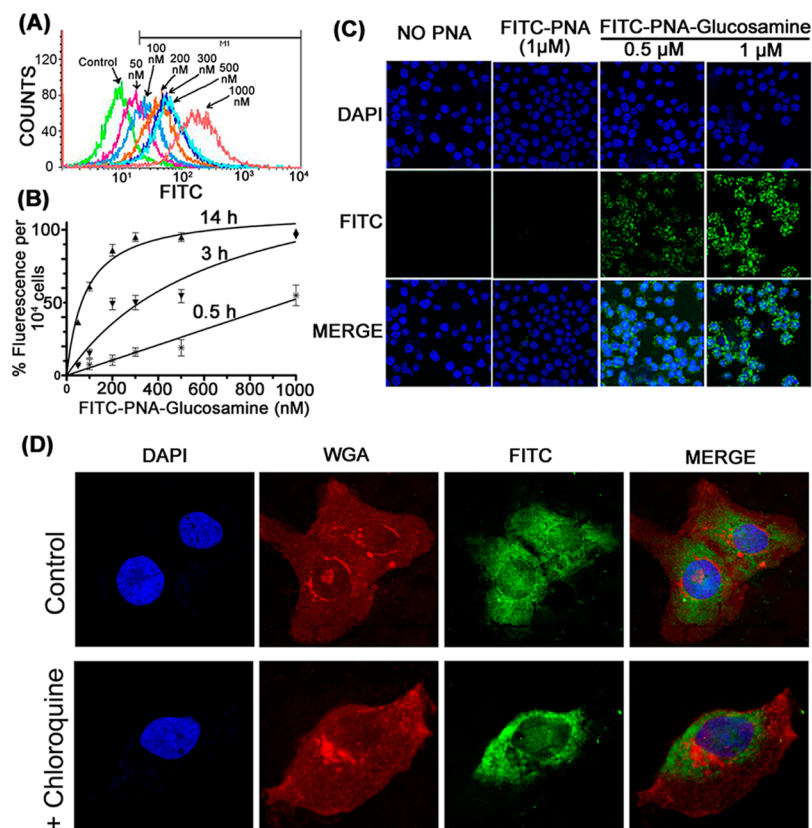


**Figure 2.** (A) Uptake of FITC labeled PNA–aminoglucosamine (**5b**) in CEM cells: cells were incubated with varying concentration of **5b** (50 nM to 1  $\mu$ M) in complete RPMI medium at 37  $^{\circ}$ C for 14 h. Cells were washed and resuspended in PBS containing 2% FBS, and fluorescence positive cells were measured by FACSscan. (B) The graphical presentation of percent uptake of **5b** as a function of time and concentration. (C) Cellular localization of FITC labeled PNA–glucosamine **5b** in CEM cells: Cells were incubated in the absence of PNA or in the presence of 1  $\mu$ M FITC labeled naked PNA or 0.5 and 1  $\mu$ M of **5b**. After 12 h, cells were washed and images were acquired. DAPI was used to stain (blue) cellular nuclei; FITC indicates the fluorescence of FITC labeled PNA or its glucosamine conjugate **5b**, measured at 488 nm. MERGE shows the distribution of **5b** in the cell. (D) Cellular localization of **5b** in Huh7.5 cells: Cells were incubated with 1  $\mu$ M of **5b** in the absence (control) and presence of chloroquine as described by Turner et al.<sup>67</sup> Images were acquired after 10 h of incubation, washing, and staining with WGA-rhodamine and DAPI to label the membrane glycoproteins (red) and nuclear DNA (blue) respectively. The FITC labeled PNA–glucosamine **5b** is shown in green fluorescence. The merge indicate superimposition of blue, red, and green.

O-4-linking arm and the N-2-trityl group. Thus **15** was used without protection of the 3-hydroxyl function for the coupling to the protected PNAs after exchange of the sodium counterion for a triethylammonium cation (Scheme 2).

This salt was coupled at the N-terminus of the protected 16-mer anti-TAR PNA **3a** attached to its solid support of synthesis using EDC/HOBT as coupling agents. Concomitant deprotection of the neosamine moiety, of the PNA bases, and cleavage from the solid support were performed in one step using TFA/anisole (1:1). The resulting conjugate **5a** was purified by HPLC on C18 reversed phase (50% coupling yield)

and its structure was confirmed by mass spectrometry (MALDI: calcd 4574.88, found 4576.00).

To study the cellular uptake of the anti-TAR PNA–neosamine conjugate, a second anti-TAR conjugate incorporating at its C-terminus extremity, a fluorescent probe was prepared from a protected lysine residue functionalized with fluorescein isothiocyanate (FITC) and attached to a solid support. For this, the neosamine derivative **15** was coupled to the protected anti-TAR PNA **3b** bearing fluorescein at the C-terminus. The resulting conjugate was deprotected and cleaved from the solid support with TFA/anisole. It was purified by

HPLC to give rise to the fluorescent conjugate **5b** (Scheme 2); its structure was confirmed by mass spectrometry (MALDI: calcd 5206.09, found 5207.28).

### ■ STABILITY OF THE PNA–GLUCOSAMINE CONJUGATE (**5a**) UNDER ACIDIC CONDITIONS

The DNA oligonucleotides based antisenses are susceptible to apurination under acidic condition and hence not suitable for oral administration. Although naked PNAs are highly stable molecule under acidic conditions, we expected that its glucosamine conjugate should also be stable under similar conditions. To examine this, we incubated **5a** with 0.1 M aqueous HCl at 37 °C for 3 days and then compared its HPLC elution profile with untreated samples. We found no difference in the retention time of treated and untreated samples and thus confirming its stability at high acidic conditions (data not shown).

### ■ CELLULAR UPTAKE, LOCALIZATION, AND ANTIVIRAL ACTIVITY

**Cellular Uptake.** Since in our earlier studies we have shown that fluorescein labeled PNA–neamine when incubated with the cells at a 2  $\mu\text{M}$  concentration, approximately 33% cells became fluorescence positive after overnight incubation.<sup>76</sup> We therefore examined if conjugate **5b** carrying one 6-aminoglucosamine ring is a better candidate for biodelivery. The CEM cells were incubated with increasing concentration of **5b** at 37 °C. Cells were harvested at different time points (30 min, 3 and 14 h) and measured for fluorescence by FACScan. We noted that **5b** is efficiently taken up by the cells in a time and concentration dependent manner (Figure 2A,B). At 0.2  $\mu\text{M}$  concentration, 10% of the cells were fluorescence positive within 30 min, which reached to 85% within 14 h (Figure 2B). By increasing the concentration to 0.3  $\mu\text{M}$ , nearly 100% cells were positive within 14 h of incubation (Figure 2B). We further noted that the cellular uptake of **5b** was independent of temperature, suggesting that its uptake is not via endocytosis, which has been shown to be temperature dependent and occurs at physiological temperature.<sup>86</sup> We observed that the extent of cellular uptake of **5b** remained unchanged at both 4 and 37 °C (results not shown). We also noted that PNA–aminoglucosamine is not cytotoxic because greater than 95% cells remained viable at all the concentrations (0.2–1  $\mu\text{M}$ ) tested. Thus, the cellular uptake of **5b** which carries only ring II of the neamine core was found to be improved several fold as compared to that observed with PNA–neamine conjugate **4**.<sup>76</sup> As against conjugate **4**, which displayed only 30% uptake at 2  $\mu\text{M}$  concentration after overnight incubation, **5b** displayed 100% cellular uptake at 0.3  $\mu\text{M}$  concentration within 14 h of incubation.

To further confirm the cellular uptake of **5b** in CEM cells, we captured the images of cells treated with FITC labeled naked PNA and FITC labeled PNA–aminoglucosamine (**5b**) using confocal microscope. The cells were incubated with the indicated amount of FITC labeled naked PNA or FITC labeled PNA–aminoglucosamine **5b**. After 12 h, cells were harvested and visualized by confocal microscope (Figure 2C). The cells incubated in the presence of 0.5 and 1  $\mu\text{M}$  of **5b** showed approximately 90% and 99% fluorescence positive cells, respectively. In contrast, FITC labeled naked PNA was unable to enter in the cell even after prolonged incubation.

It has been recognized that cellular delivery of PNAs conjugated with cell penetrating peptides occurs mainly through endocytotic pathways and thus retaining a major fraction of internalized PNA in the endosome–lysosome compartments.<sup>87</sup> Endosome disrupting agents such as chloroquine have shown to improve the release of the endosomal entrapped PNA into the cytosol. Confocal microscopy studies carried out by Turner et al.<sup>67</sup> have demonstrated that fluorescently labeled PNA–peptide conjugates sequestered in endosomes or membrane-bound compartments in HeLa cells are significantly reduced when cotreated with chloroquine and thus result in improved distribution of the conjugates in the cytosol.<sup>67</sup>

We therefore resorted to examine if there is any difference in the cellular distribution of **5b** upon cotreatment with chloroquine. We used Huh7.5 cells, which have much larger cytoplasmic space as compared to CEM cells, and incubated these cells with 1  $\mu\text{M}$  of the conjugate **5b** in the absence and presence of chloroquine as described before.<sup>67</sup> After 10 h of incubation, cells were washed by PBS and fixed with 4% paraformaldehyde. The cellular nucleus and the membrane glycoproteins were stained by DAPI and wheat germ agglutinin conjugated with rhodamine (WGA), respectively, and examined by confocal microscopy. The result shown in Figure 2D indicates that cellular distribution of **5b** remained unaffected upon cotreatment with chloroquine, suggesting the absence of endosomal entrapment of **5b** in the cell.

This result is exciting because most of the biodelivery system so far developed for PNA have limitations due to their endosomal entrapment in the cytosol.<sup>67</sup> Our results with **5b** indicate that the problem associated due to endosomal compartmentalization could be circumvented by conjugating target specific PNA to the 6-aminoglucosamine ring. The localization and distribution of **5b** in both cytosol and nucleus indicate that **5a** could efficiently block Tat mediated transactivation of HIV-1 transcription in the nucleus and abort reverse transcription process of viral RNA in the cytosol.

### ■ TARGET SPECIFICITY

Because cellular uptake of PNA conjugated with 6-aminoglucosamine was significantly enhanced, we examined if this improvement in uptake is not compromised by target specificity. We then examined the binding specificity of the PNA–aminoglucosamine conjugate (**5a**) to the TAR RNA by gel mobility shift assay using the <sup>32</sup>P-labeled 82 bp long TAR RNA transcript. We also used mutated TAR RNA carrying a deletion in the stem (TAR-BS) and a 98 base long RNA fragment from hepatitis C virus 3' nontranslated region (HCV-3'NTR) as the nontarget RNA and scrambled PNA–glucosamine as the negative controls. As shown in Figure 3, a distinct shift in the mobility of TAR RNA was observed due to the formation of PNA–RNA complex. The extent of gel shift of the target RNA by **5a** was stoichiometric. At 0.5:1 molar ratio of **5a** to TAR RNA, 50% gel shift was seen while complete shift was noted at 1:1 molar ratio (lane 5). We have earlier demonstrated that PNA–neamine conjugate **4** exhibits metal independent RNA nuclease activity which specifically cleaves the target RNA at the binding site upon prolonged incubation.<sup>75</sup> However, we could not demonstrate similar target specific RNA cleavage activity with conjugate **5a** either in the absence or presence of different metals ions (results not shown).

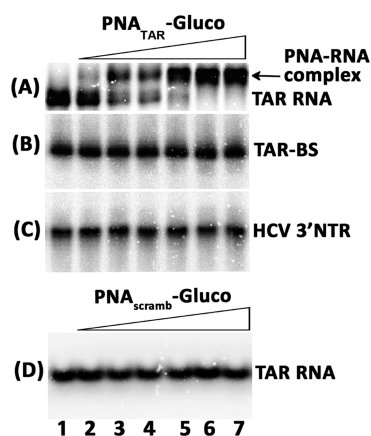


**Figure 3.** (A) Binding specificity of PNATAR–aminoglucosamine (conjugate **5a**) to its target sequence. The affinity of the conjugate **5a** (A) for its target sequence on the TAR RNA was assessed by gel mobility shift analysis. (B) TAR mutant RNA carrying a deletion at the top of the stem (TAR BS). (C) The 98-mer HCV 3'NTR RNA fragment as the nontarget RNA. (D) TAR RNA incubated with scrambled PNA–glucosamine conjugate **5a** as a negative control. Lane 1 through 7 represents molar ratios of PNA<sub>TAR</sub>–glucosamine or scrambled PNA–aminoglucosamine to TAR RNA of 0.0, 0.2, 0.5, 0.8, 1.0, 2.0, and 5.0, respectively.

### ■ INHIBITION OF TAT-MEDIATED TRANSACTIVATION OF HIV-1-LTR

Because the PNA–glucosamine conjugate **5a** targeted to HIV-1 TAR is efficiently taken up by the cells, we examine if **5a** is able to block Tat-mediated transactivation of transcription of HIV-1 long terminal repeat (HIV-1 LTR) when supplemented in the culture medium. The significance of Tat–TAR interaction in regulating HIV-1 gene expression is well documented.<sup>88,89</sup>

Activation of transcriptional elongation occurs following the recruitment of Tat to the transcription machinery via a specific interaction with TAR, a 59-residue RNA leader sequence in the HIV-1 LTR.<sup>89</sup> The main advantage of targeting the TAR element is that it is conserved and folds into a stable stem–loop structure. It was expected that binding of **5a** to sequences on the stem–loop region of TAR may destabilize the stem–loop structure of TAR and abolish Tat–TAR interaction. If this mode of action is the case, then **5a** should be able to negatively impact Tat/LTR driven reporter while should have no effect in the absence of Tat.

To examine this, we used a reporter plasmid construct (pHIV-1 LTR-Luc) expressing firefly luciferase under the control of the HIV-1 LTR and pRL-SV40 expressing *Renilla* luciferase under the control of SV40 as an internal control. The reporter plasmids were cotransfected in CEM cells with and without pCMV-Tat. The transfected cells were grown in RPMI medium supplemented with or without different concentrations of **5a** or scrambled PNA–glucosamine conjugate. After 24 h, cells were harvested, lysed, and assayed for the determination of relative expression of firefly and *Renilla* luciferase activity (Figure 4). Expression of *Renilla* luciferase driven by the CMV promoter did not change in the absence or presence of the Tat expression clone or in the presence or absence of **5a** and was therefore used as a control to normalize for transfection efficiency. On the other hand, expression of the firefly luciferase driven by the HIV-1 LTR directly correlated with the concentration of **5a**, thus indicating its promoter specificity. These results are presented in Figure 4 as the percent inhibition of Tat-mediated transactivation of the HIV-1 LTR at indicated concentrations of **5a** or scrambled PNA–glucosamine conjugate calculated from the respective ratios of the firefly and *Renilla* luciferase activities.

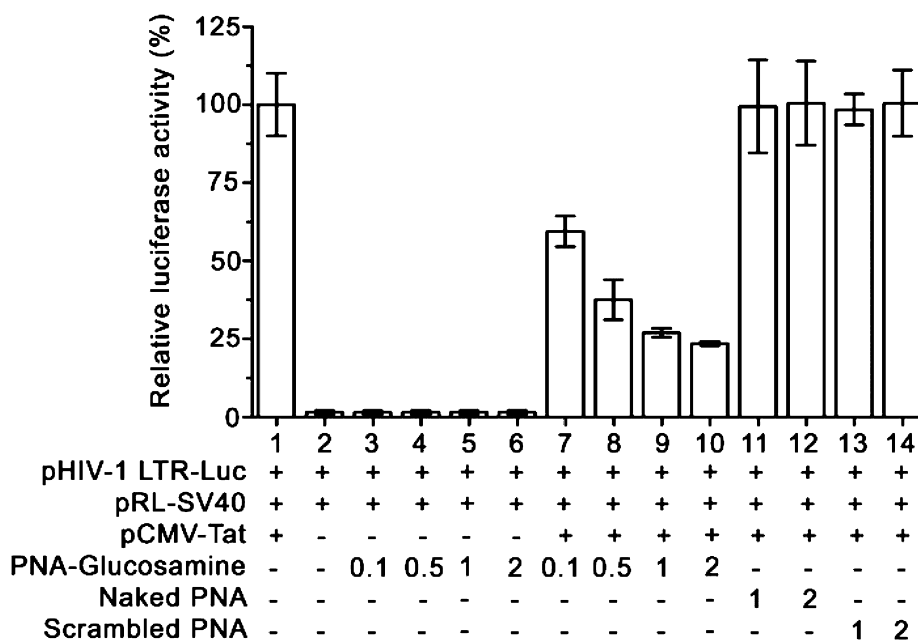


**Figure 4.** Effect of the PNA–glucosamine conjugate **5a** on Tat-mediated transactivation: CEM cells ( $0.5 \times 10^6$  cells per well in 12 well plate) were transfected with the reporter plasmids pHIV-1 LTR-Luc ( $2 \mu\text{g}$ ) and pRL-SV40 ( $500 \text{ ng}$ ) in the presence and absence of Tat expression vector, pCMV-Tat ( $2 \mu\text{g}$ ). After 2 h of transfection, cells were supplemented with PNA conjugates in the concentration as indicated in  $\mu\text{M}$ . The transfected cells were harvested 24 h post-transfection, and the luciferase activities were measured. Expression of *Renilla* luciferase was considered as a control for normalization of transfection efficiency. The results are presented as the relative ratio of firefly to *Renilla* luciferase activity in percentage by keeping the relative activity of untreated cells as 100%. Error bars represent the standard error of the mean of two independent experiments.

As shown in Figure 4, relative luciferase activity was barely detectable in the absence of Tat (lane 2) as compared to that observed in the presence of Tat (lane 1). The expression of firefly luciferase was strongly inhibited when transfected cells were grown in the presence of **5a** (lanes 7–10). Approximately 75% inhibition of Tat-mediated transactivation of firefly luciferase was noted at 1  $\mu\text{M}$  concentration of **5a**. In contrast, only a basal level of LTR driven firefly luciferase expression was observed in the absence of Tat (lane 2), which remained unaffected by **5a** (lanes 3–6).

The naked PNA (lanes 11, 12) or scrambled PNA–glucosamine conjugate (lanes 13, 14) had no effect on the expression of firefly luciferase when supplemented in the culture medium. These results clearly indicated that **5a** effectively blocks Tat-mediated transactivation of the HIV-1 LTR.

### ANTIVIRAL ACTIVITY AND CYTOTOXICITY

Because PNA–aminoglucosamine conjugate efficiently internalized in the cell and binds the target sequence in HIV-1 TAR RNA, we examined if the conjugate is able to block TAR mediated transactivation of HIV-1 transcription in HIV-1 infected lymphocytes. To evaluate this, we used pseudotyped HIV-1 particles carrying luciferase reporter gene to infect CEM T-lymphocyte cells. The infected cells were grown at 37 °C for 48 h and then supplemented with increasing concentration of **5a**. After 76 h, cells were lysed and assayed for firefly luciferase activity. The results shown in Figure 5 indicate that **5a** strongly

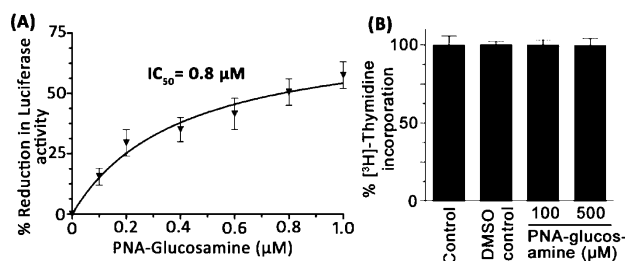


**Figure 5.** (A) Inhibition of HIV-1 transcription by **5a**: The CEM cells were infected with pseudotyped HIV-1 virus expressing the firefly luciferase reporter. After 48 h postinfection, indicated amount of PNA–aminoglucosamine was supplemented in the culture medium. After 76 h, cells were harvested and assayed for firefly luciferase activity in the cell extract. The results are expressed as mean value of two independent experiments with error bar. (B) Effect of **5a** on cellular proliferation: CEM cells were grown in the absence or presence of 0.1 mM and 0.5 mM of **5a** dissolved in DMSO. The final concentration of DMSO supplemented through **5a** in the medium was 5%. The culture medium was supplemented with 5  $\mu\text{Ci}$  of [methyl- $^3\text{H}$ ]thymidine/mL. After 48 h, cells were harvested and [ $^3\text{H}$ ]–thymidine incorporated into the DNA was determined. The results expressed as percent of thymidine incorporation with respect to the control are the averages of three sets of independent experiments.

inhibited HIV-1 transcription by blocking the TAR, as evident by the low level of expression of luciferase activity. Approximately 50% reduction in luciferase activity was observed at 800 nM concentration of **5a**. We further confirmed that dose-dependent reduction in luciferase expression is not due to cellular cytotoxicity of **5a**. As shown in Figure 5B, we did not find any difference in the [ $^3\text{H}$ ]thymidine incorporation when infected CEM cells were grown in the absence or presence of indicated concentration of PNA–aminoglucos-

amine. The cells grown in the presence of 0.1 and 0.5 mM PNA–aminoglucosamine (**5a**) showed similar extent of [ $^3\text{H}$ ]thymidine incorporation, suggesting that the cellular proliferation was not affected in the presence of **5a**.

### CONCLUSION

In conclusion, the PNA–aminoglucosamine conjugate **5a** carrying a reduced number of amino groups as compared to the PNA–neamine conjugate **4** displayed several-fold enhanced cellular uptake and target efficacy at subnanomolar concentration. It efficiently enters the cells, strongly binds to its target sequence on HIV-1 genome, blocks Tat-mediated transactivation of HIV-1 LTR, and inhibits virus production in HIV-1 infected cells. The most exciting results was that, unlike peptide based PNA biodelivery system, PNA conjugated with glucosamine is uniformly localized and distributed in the cytosol and nucleus and not subjected to endosomal compartment in the cytosol. Using this novel class of small molecule to conjugate sequence specific PNA for sequestering critical regulatory elements in the viral RNA genome may have great potential in PNA based therapeutics. A strategy to enhance oral biodelivery of PNAs will certainly improve their therapeutic because PNA–aminoglucosamine conjugates being highly stable under acidic conditions corresponding to the stomachal environment may also be expected to be compatible with oral administration.

### EXPERIMENTAL SECTION

**General.** All reagents were used as purchased from suppliers without further purification. The protected 16-mer PNA oligomers were purchased from Eurogentec. DMF was distilled in the presence of  $\text{CaH}_2$  and stored under argon atmosphere prior to use. Thin layer chromatographies were performed on silica gel (Alugram Sil G/UV $_{254}$ ) or alumina gel (Alugram Alox N/UV $_{254}$ ) from Macherey-Nagel, and spots were detected either by UV absorption or by charring with ninhydrin. HPLC purifications were carried out on a  $\text{C}_{18}$  reversed-phase column (Macherey-Nagel, 10.0 mm  $\times$  25.0 mm) with a Dionex Ultimate 3000 apparatus. Melting points were determined with a BUCHI 510 apparatus and are reported uncorrected.  $^1\text{H}$  NMR (400 MHz) and  $^{13}\text{C}$  NMR (100 MHz) spectra were recorded with a BRUKER ADVANCE 400 spectrometer using the residual solvent signal as internal standard. HRMS were obtained from the Mass Spectrometry Service, CRMPO, at the University of Rennes I, France, using a MICROMASS ZABSPEC-TOF spectrometer and a VARIAN MAT311 spectrometer or with a 4700 reflector spectrometer. The purities of the conjugates **5a** and **5b** determined by  $\text{C}_{18}$  reversed phase HPLC were found to be 96.2% and 98.5%, respectively (see Supporting Information).

**Synthesis. Glucosamine Derivative 7.** To a solution of compound **6**<sup>84</sup> (3.30 g, 10.7 mmol) in dry DMF (15 mL) were added successively  $\text{K}_2\text{CO}_3$  (7.4 g, 54 mmol, 5 equiv) and benzyl bromide (3.18 mL, 26.7 mmol, 2.5 equiv). The solution was stirred at room temperature for 10 h under argon atmosphere. A saturated  $\text{NH}_4\text{Cl}$  solution was added, and the mixture was extracted with ethyl acetate (3  $\times$  20 mL). The combined organic layers were dried over  $\text{MgSO}_4$ , filtered, and concentrated. The residue obtained was purified over silica gel column (EtOAc/cyclohexane, 1/3) to afford **7** (3.57 g, 84%) as a white solid; mp 186–188 °C.  $^1\text{H}$  NMR (400 MHz,  $\text{CDCl}_3$ )  $\delta$  3.19 (s, 3H, OMe), 3.35 (dd,  $J$  = 12.0 Hz, 1H, H-2), 3.78–3.85 (m, 2H, H-5, H-6'), 3.98 (q,  $J$  = 8.0, 12.0 Hz, 1H, H-4), 4.21–4.24 (m, 1H, H-6), 4.45 (s, 2H,  $\text{NCH}_2\text{Ph}$ ), 4.58 (d,  $J$  = 4.0 Hz, 1H, H-1), 4.69 (q,  $J$  = 8.0, 12.0 Hz, 1H, H-3), 5.57 (s, 1H,  $\text{CHPh}$ ), 7.33–7.38 (m, 8H, aromatic), 7.47–7.49 (m, 2H, aromatic).  $^{13}\text{C}$  NMR (100 MHz,  $\text{CDCl}_3$ )  $\delta$  49.0 ( $\text{NCH}_2\text{Ph}$ ), 55.8 (OMe), 62.3 (C-2), 65.6 (C-5), 68.7 (C-6), 73.2 (C-3), 80.4 (C-4), 97.4 (C-1), 101.6 ( $\text{CHPh}$ ), 126.3, 128.5, 128.9, 129.0, 129.2, 129.4, 135.3, 136.7, 158.9 (CO). HRMS (ESI) Calcd for  $\text{C}_{22}\text{H}_{23}\text{NO}_6\text{Na}$  [M

+ Na]<sup>+</sup>: 420.14231, found 420.1411, Calcd for C<sub>22</sub>H<sub>23</sub>NO<sub>6</sub>K [M + K]<sup>+</sup>: 436.1162, found 436.1160.

**Glucosamine Derivative 8.** To a stirred solution of compound 7 (2.20 g, 5.54 mmol) in dry dichloromethane (10 mL), under argon atmosphere, was added Et<sub>3</sub>SiH (5.47 mL, 66.5 mmol, 12 equiv), and the mixture was cooled to 0 °C. To this mixture, BF<sub>3</sub>·OEt<sub>2</sub> (1.39 mL, 11.08 mmol, 2 equiv) was added dropwise, and then the reaction mixture was stirred at 0 °C for 2 h. A saturated NaHCO<sub>3</sub> solution was added, and the resulting aqueous mixture was extracted with dichloromethane (3 × 20 mL). The combined organic layers were dried over MgSO<sub>4</sub>, filtered, and concentrated. The residue was purified over silica gel column (EtOAc/cyclohexane, 1/1) to afford 8 (1.79 g, 81%) as a yellow foam. <sup>1</sup>H NMR (400 MHz, CD<sub>3</sub>OD) δ 3.13 (s, 3H, OMe), 3.34 (dd, J = 4.0, 8.0 Hz, 1H, H-2), 3.57–3.61 (m, 1H, H-5), 3.72–3.73 (m, 2H, H-6, H-6'), 3.89 (t, J = 8.0 Hz, 1H, H-4), 4.29 (d, J = 12.0 Hz, 1H, NCH<sub>2</sub>Ph), 4.37–4.57 (m, 4H, H-3, OCH<sub>2</sub>Ph, NCH<sub>2</sub>Ph), 4.61 (d, J = 4.0 Hz, 1H, H-1), 7.31–7.36 (m, 10H, aromatic). <sup>13</sup>C NMR (100 MHz, CD<sub>3</sub>OD) δ 49.5 (NCH<sub>2</sub>Ph), 55.9 (OMe), 62.8 (C-2), 69.7 (C-4), 69.9 (C-6), 74.5 (OCH<sub>2</sub>Ph), 75.7 (C-5), 78.4 (C-3), 97.7 (C-1), 128.8, 128.9, 129.1, 129.5, 129.7, 129.8, 137.1, 139.6, 161.4 (CO). HRMS (ESI) Calcd for C<sub>22</sub>H<sub>23</sub>NO<sub>6</sub>Na [M + Na]<sup>+</sup>: 422.1580, found 422.1587. Calcd for C<sub>22</sub>H<sub>23</sub>NO<sub>6</sub>K [M + K]<sup>+</sup>: 438.1319, found 438.1299.

**Glucosamine Derivative 9.** To a solution of compound 8 (2.80 g, 7.01 mmol) in DMF (10 mL) was added NaH (0.56 g, 14.02 mmol, 2 equiv, 60% suspension), and the mixture was stirred at room temperature for 10 min under argon atmosphere. Ethyl 6-bromo hexanoate (2.61 mL, 14.02 mmol, 2 equiv) was added, and the mixture was stirred at room temperature for 8 h. A saturated NH<sub>4</sub>Cl solution was added, and the resulting aqueous mixture was extracted with ethyl acetate (3 × 20 mL). The combined organic layers were dried over anhydrous MgSO<sub>4</sub>, filtered, and concentrated. The residue was purified over silica gel column (EtOAc/cyclohexane, 1/3) to afford 9 (3.49 g, 92%) as a yellow foam. <sup>1</sup>H NMR (400 MHz, CDCl<sub>3</sub>) δ 1.26 (t, J = 8.0 Hz, 3H, Me), 1.27–1.31 (m, 2H, H-3'), 1.45–1.49 (m, 2H, H-2'), 1.59–1.62 (m, 2H, H-4'), 2.27 (t, J = 8.0 Hz, 2H, CH<sub>2</sub>CO), 3.15 (s, 3H, OMe), 3.27 (dd, J = 4.0, 12.0 Hz, 1H, H-2), 3.36–3.37 (m, 1H, OCH<sub>2</sub>), 3.58–3.61 (m, 2H, H-5, H-6'), 3.68–3.71 (m, 2H, H-4, H-6), 3.78 (m, 1H, OCH<sub>2</sub>), 4.13 (q, J = 8.0, 16.0 Hz, 2H, CH<sub>2</sub>-ethyl ester), 4.41 (d, 2H, NCH<sub>2</sub>Ph), 4.45–4.52 (m, 2H, H-3, OCH<sub>2</sub>Ph), 4.55 (d, J = 4.0 Hz, 1H, H-1), 4.63 (d, J = 12.0 Hz, 1H, OCH<sub>2</sub>Ph), 7.29–7.37 (m, 10H, aromatic). <sup>13</sup>C NMR (100 MHz, CDCl<sub>3</sub>) δ 14.4 (Me), 24.9 (C-4'), 25.7 (C-3'), 29.7 (C-2'), 34.4 (CH<sub>2</sub>CO), 48.9 (NCH<sub>2</sub>Ph), 55.6 (OMe), 60.4 (CH<sub>2</sub>-ethyl ester), 61.3 (C-2), 67.9 (C-6), 71.3 (OCH<sub>2</sub>), 72.7 (C-5), 73.7 (OCH<sub>2</sub>Ph), 75.5 (C-4), 77.4 (C-3), 96.4 (C-1), 127.9, 128.0, 128.4, 128.6, 128.9, 135.4, 138.0, 159.3 (CO-amide), 173.8 (CO-ester). HRMS (ESI) Calcd for C<sub>30</sub>H<sub>39</sub>NO<sub>8</sub>Na [M + Na]<sup>+</sup>: 564.2573, found 564.2574. Calcd for C<sub>30</sub>H<sub>39</sub>NO<sub>8</sub>K [M + K]<sup>+</sup>: 580.2313, found 580.2345. Calcd. for C<sub>29</sub>H<sub>39</sub>NO<sub>6</sub>Na [M - CO<sub>2</sub> + Na]<sup>+</sup>: 520.2675, found 520.2688.

**Glucosamine Derivative 10.** To a solution of compound 9 (3.20 g, 5.91 mmol) in a MeOH/H<sub>2</sub>O (9/1 mL) mixture were added Pd(OH)<sub>2</sub>/C (20%) (0.17 g, 1.18 mmol, 0.2 equiv) and HCO<sub>2</sub>NH<sub>4</sub> (1.86 g, 29.5 mmol, 5 equiv). The resulting mixture was refluxed for 1.5 h, filtered through a pad of Celite, and concentrated. The residue was purified over silica gel column (EtOAc/pentane, 2/1) to afford 10 (2.61 g, 98%) as a yellow foam. <sup>1</sup>H NMR (400 MHz, CDCl<sub>3</sub>) δ 1.25 (t, J = 8.0 Hz, 3H, Me), 1.36–1.38 (m, 2H, H-4'), 1.55–1.65 (m, 4H, H-2', H-3'), 2.29 (t, J = 8.0 Hz, 2H, CH<sub>2</sub>CO), 3.15 (s, 3H, OMe), 3.21 (dd, J = 12 Hz, 1H, H-2), 3.49–3.53 (m, 2H, H-5, OCH<sub>2</sub>), 3.67 (t, J = 8.0 Hz, 1H, H-4), 3.76 (d, 2H, H-6, H-6'), 3.83–3.87 (m, 1H, OCH<sub>2</sub>), 4.12 (q, J = 8.0, 16.0 Hz, 2H, CH<sub>2</sub>-ethyl ester), 4.41 (d, 2H, NCH<sub>2</sub>Ph), 4.50–4.55 (m, 2H, H-1, H-3), 7.30–7.36 (m, 5H, aromatic). <sup>13</sup>C NMR (100 MHz, CDCl<sub>3</sub>) δ 14.2 (Me), 24.6 (C-4'), 25.5 (C-3'), 29.4 (C-2'), 34.2 (CH<sub>2</sub>CO), 48.6 (NCH<sub>2</sub>Ph), 55.4 (OMe), 60.2 (CH<sub>2</sub>-ethyl ester), 61.0 (C-6), 61.2 (C-2), 71.0 (OCH<sub>2</sub>), 73.3 (C-5), 75.4 (C-4), 77.1 (C-3), 96.2 (C-1), 128.2, 128.6, 128.7, 135.2, 159.1 (CO, amide), 173.8 (CO, ester). HRMS (ESI) Calcd for C<sub>23</sub>H<sub>33</sub>NO<sub>8</sub>Na [M + Na]<sup>+</sup>: 474.2104, found 474.2117. Calcd for C<sub>23</sub>H<sub>34</sub>NO<sub>8</sub> [M + H]<sup>+</sup>: 452.2284, found, 452.2284.

**Glucosamine Derivative 11.** To a solution of compound 10 (1.60 g, 3.54 mmol) in dry pyridine (10 mL) was added TsCl (1.69 g, 8.85 mmol, 2.5 equiv), and the mixture was stirred at ambient temperature under argon atmosphere. After completion of the reaction (TLC), saturated NaHCO<sub>3</sub> solution was added and the resulting aqueous mixture was extracted with ethyl acetate (3 × 10 mL). The combined organic layers were dried over anhydrous MgSO<sub>4</sub>, filtered, and concentrated. The residue was purified over silica gel column (EtOAc/pentane, 1/2) to afford the desired compound 11 (2.06 g, 96%) as a yellow oil. <sup>1</sup>H NMR (400 MHz, CDCl<sub>3</sub>) δ 1.25 (t, J = 8.0 Hz, 3H, Me), 1.27–1.30 (m, 2H, H-3'), 1.41–1.46 (m, 2H, H-2'), 1.57–1.61 (m, 2H, H-4'), 2.26 (t, J = 8.0 Hz, 2H, CH<sub>2</sub>CO), 2.43 (s, 3H, Me), 3.05 (s, 3H, OMe), 3.17 (dd, J = 4.0, 12.0 Hz, 1H, H-2), 3.31–3.33 (m, 1H, OCH<sub>2</sub>), 3.54–3.57 (m, 2H, H-4, H-5), 3.74–3.77 (m, 1H, OCH<sub>2</sub>), 4.12 (q, J = 8.0, 16.0 Hz, 2H, CH<sub>2</sub>-ethyl ester), 4.16 (d, J = 4.0 Hz, 1H, H-6'), 4.24 (dd, J = 4.0, 8.0 Hz, 1H, H-6), 4.30 (d, J = 16.0 Hz, 1H, NCH<sub>2</sub>Ph), 4.40–4.47 (m, 3H, H-1, H-3, NCH<sub>2</sub>), 7.27–7.34 (m, 7H, aromatic), 7.75 (d, J = 8.0 Hz, 2H, aromatic). <sup>13</sup>C NMR (100 MHz, CDCl<sub>3</sub>) δ 14.4 (Me), 21.8 (Me), 24.8 (H-4'), 25.6 (H-3'), 29.6 (H-2'), 34.3 (CH<sub>2</sub>CO), 48.9 (NCH<sub>2</sub>Ph), 55.7 (OMe), 60.3 (CH<sub>2</sub>-ethyl ester), 61.2 (C-2), 68.1 (C-6), 70.9 (C-5), 71.2 (OCH<sub>2</sub>), 75.2 (C-4), 76.8 (C-3), 96.3 (C-1), 128.1, 128.4, 128.6, 128.8, 128.9, 130.0, 133.0, 135.2, 145.1, 158.9 (CO-amide), 173.7 (CO-ester). HRMS (ESI) Calcd for C<sub>30</sub>H<sub>39</sub>NO<sub>10</sub>NaS [M + Na]<sup>+</sup>: 628.2192, found 628.2187. Calcd for C<sub>30</sub>H<sub>39</sub>NO<sub>10</sub>SK [M + K]<sup>+</sup>: 644.1932, found 644.1927.

**Glucosamine Derivative 12.** To a solution of compound 11 (1.90 g, 3.14 mmol) in DMF (10 mL) was added NaN<sub>3</sub> (2.04 g, 31.4 mmol, 10 equiv), and then the solution was heated at 80 °C for 3 h under argon atmosphere. A saturated NH<sub>4</sub>Cl solution was added, and the resulting aqueous mixture was extracted with ethyl acetate (3 × 10 mL). The combined organic layers were dried over anhydrous MgSO<sub>4</sub>, filtered, and concentrated under reduced pressure. The residue was purified over a silica gel column (EtOAc/pentane, 1/3) to afford 12 (1.36 g, 91%) as a yellow gummy liquid. <sup>1</sup>H NMR (400 MHz, CDCl<sub>3</sub>) δ 1.24 (t, J = 8.0 Hz, 3H, Me), 1.32–1.36 (m, 2H, H-3'), 1.53–1.56 (m, 2H, H-2'), 1.58–1.64 (m, 2H, H-4'), 2.28 (t, J = 8.0 Hz, 2H, CH<sub>2</sub>CO), 3.13 (s, 3H, OMe), 3.24 (dd, J = 4.0, 12.0 Hz, 1H, H-2), 3.43–3.47 (m, 3H, H-6, H-6', OCH<sub>2</sub>), 3.55 (t, J = 8.0, 12.0 Hz, 1H, H-4), 3.62–3.65 (m, 1H, H-5), 3.81–3.87 (m, 1H, OCH<sub>2</sub>), 4.11 (q, J = 8.0, 16.0 Hz, 2H, CH<sub>2</sub>-ethyl ester), 4.34 (d, J = 16.0 Hz, 1H, NCH<sub>2</sub>Ph), 4.45–4.51 (m, 3H, H-1, H-3, NCH<sub>2</sub>), 7.30–7.36 (m, 5H, aromatic). <sup>13</sup>C NMR (100 MHz, CDCl<sub>3</sub>) δ 14.4 (Me), 24.8 (H-4'), 25.7 (H-3'), 29.6 (H-2'), 34.3 (CH<sub>2</sub>CO), 48.9 (NCH<sub>2</sub>Ph), 51.0 (C-6), 55.7 (OMe), 60.4 (CH<sub>2</sub>-ethyl ester), 61.5 (C-2), 71.2 (OCH<sub>2</sub>), 72.5 (C-5), 76.5 (C-4), 76.9 (C-3), 96.3 (C-1), 128.4, 128.8, 128.9, 135.3, 159.0 (CO-amide), 173.7 (CO-ester). HRMS (ESI) Calcd for C<sub>23</sub>H<sub>32</sub>N<sub>4</sub>O<sub>7</sub>Na [M + Na]<sup>+</sup>: 499.2169, found 499.2183. Calcd for C<sub>23</sub>H<sub>32</sub>N<sub>4</sub>O<sub>7</sub>K [M + K]<sup>+</sup>: 515.1908, found 515.1916.

**Glucosamine Derivative 13.** A solution of compound 12 (1.10 g, 2.31 mmol) in a mixture of 1 M NaOH/1,4-dioxane (5/5 mL, v/v) was heated at 80 °C for 20 h. The mixture was diluted with ethyl acetate and washed with brine. The separated aqueous layer was repeatedly washed with ethyl acetate. The combined organic layers were dried over anhydrous MgSO<sub>4</sub>, filtered, and concentrated. The residue obtained was purified over a silica gel column (CH<sub>2</sub>Cl<sub>2</sub>/MeOH, 9/1) to afford 13 (0.72 g, 74%) as a yellow gummy liquid. <sup>1</sup>H NMR (400 MHz, CDCl<sub>3</sub>) δ 1.37–1.43 (m, 2H, H-3'), 1.53–1.64 (m, 4H, H-2', H-4'), 2.30 (t, J = 4.0, 8.0 Hz, 2H, CH<sub>2</sub>CO), 2.70 (dd, J = 4.0, 12.0 Hz, 1H, H-2), 3.13 (t, J = 8.0 Hz, 1H, H-4), 3.31 (s, 3H, OMe), 3.40 (dd, J = 8.0, 12.0 Hz, 1H, H-6'), 3.48 (dd, J = 12.0 Hz, 1H, H-6), 3.51–3.55 (m, 1H, OCH<sub>2</sub>), 3.62–3.66 (m, 1H, H-5), 3.76 (t, J = 8.0, 12.0 Hz, 1H, H-3), 3.88–3.94 (m, 1H, OCH<sub>2</sub>), 3.96 (s, 2H, NCH<sub>2</sub>Ph), 4.59 (d, J = 4.0 Hz, 1H, H-1), 6.63 (bs, NH), 7.32–7.37 (m, 5H, aromatic). <sup>13</sup>C NMR (100 MHz, CDCl<sub>3</sub>) δ 24.9 (C-4'), 25.6 (C-3'), 30.0 (C-2'), 35.2 (CH<sub>2</sub>CO), 51.6 (NCH<sub>2</sub>Ph), 51.7 (C-6), 55.5 (OMe), 61.6 (C-2), 70.2 (C-5), 72.2 (C-3), 72.3 (OCH<sub>2</sub>), 78.9 (C-4), 97.1 (C-1), 128.2, 128.8, 129.0, 137.6, 179.5 (CO). HRMS (ESI) calcd. for C<sub>20</sub>H<sub>30</sub>N<sub>4</sub>O<sub>6</sub>Na [M + Na]<sup>+</sup>: 445.2069, found 445.2063.



Calcd for  $C_{20}H_{31}N_4O_6$   $[M + H]^+$ : 423.2239, found 423.2244. Calcd for  $C_{19}H_{27}N_4O_5$   $[M - CH_3OH + H]^+$ : 391.1981, found 391.1972.

**Glucosamine Derivative 14.** To a solution of compound 13 (0.64 g, 1.44 mmol) in a MeOH/H<sub>2</sub>O (9/1 mL) mixture were added Pd(OH)<sub>2</sub>/C (20%) (0.04 g, 0.29 mmol, 0.2 equiv) and HCO<sub>2</sub>NH<sub>4</sub> (0.45 g, 7.20 mmol, 5 equiv). The mixture was refluxed for 1.5 h, filtered through a pad of Celite, and concentrated to afford 14 (0.45 g, 95%) as a white crystalline solid; mp 87–89 °C. <sup>1</sup>H NMR (400 MHz, D<sub>2</sub>O) δ 1.30–1.35 (m, 2H, H-4'), 1.51–1.60 (m, 4H, H-2', H-3'), 2.16 (t, *J* = 8.0 Hz, 2H, CH<sub>2</sub>CO), 2.93 (dd, *J* = 4.0, 12.0 Hz, 1H, H-2), 3.11–3.22 (m, 2H, H-4, H-6'), 3.37 (dd, *J* = 4.0, 12.0 Hz, 1H, H-6), 3.40 (s, 3H, OMe), 3.61–3.70 (m, 2H, H-3, OCH<sub>2</sub>), 3.81–3.87 (m, 2H, H-5, OCH<sub>2</sub>), 4.85 (s, 1H, H-1). <sup>13</sup>C NMR (100 MHz, D<sub>2</sub>O) δ 25.0 (C-4'), 25.4 (C-3'), 28.9 (C-2'), 37.3 (CH<sub>2</sub>CO), 40.3 (C-6), 54.4 (C-2), 55.4 (OMe), 67.1 (C-5), 72.0 (C-3), 73.1 (OCH<sub>2</sub>), 79.7 (C-4), 98.5 (C-1), 183.6 (CO). HRMS (ESI) Calcd for  $C_{13}H_{26}N_2O_6Na$   $[M + Na]^+$ : 329.1689, found 329.1690. Calcd for  $C_{13}H_{27}N_2O_6$   $[M + H]^+$ : 307.1869, found 307.1864. Calcd for  $C_{13}H_{25}N_2O_6Na_2$   $[M - H + 2Na]^+$ : 351.1508, found 351.1516.

**Glucosamine Derivative 15.** A solution of compound 14 (0.22 g, 0.67 mmol) in a DMF/triethylamine (7/1 mL) mixture, under argon atmosphere, was stirred at room temperature for 30 min, and then a solution of trityl chloride (0.93 g, 3.35 mmol, 5 equiv) in a DMF/triethylamine (5/1) mixture was added. The resulting solution was stirred at room temperature for 8 h. A saturated NH<sub>4</sub>Cl solution was added, and the resulting aqueous mixture was extracted with ethyl acetate (3 × 10 mL). The combined organic layers were dried over anhydrous MgSO<sub>4</sub>, filtered, and concentrated. The residue obtained was purified over silica gel column (EtOAc/cyclohexane, 1/8 containing triethylamine) to give the tritrylated compound (0.47 g, 68%) as a white amorphous solid. HRMS (ESI) Calcd for  $C_{70}H_{69}N_2O_6$   $[M + H]^+$ : 1033.5156, found 1033.5163.

A solution of this compound (0.45 g, 0.43 mmol) in a mixture 1 M NaOH/dioxane (4/4 mL, v/v) was heated at 80 °C for 6 h and then diluted with ethyl acetate and washed with a saturated solution of NaCl. The separated aqueous layer was repeatedly washed with ethyl acetate. The combined organic layers were dried over anhydrous MgSO<sub>4</sub>, filtered, and concentrated. The obtained residue was purified over silica gel column deactivated with triethylamine (CH<sub>2</sub>Cl<sub>2</sub>/MeOH, 9/1) to give 15 (0.33 g, 85%) as a white crystalline solid; mp 107–109 °C. <sup>1</sup>H NMR (400 MHz, CDCl<sub>3</sub>) δ 1.21–1.27 (m, 2H, H-4'), 1.30 (t, *J* = 4.0, 8.0 Hz, 9H, Et<sub>3</sub>N), 1.41–1.44 (m, 2H, H-3'), 1.55–1.57 (m, 2H, H-2'), 1.97–1.98 (m, 1H, H-6'), 2.19 (t, *J* = 8.0 Hz, 2H, CH<sub>2</sub>CO), 2.50–2.53 (m, 1H, H-6), 2.77 (d, *J* = 4.0 Hz, 1H, H-1), 2.81 (dd, *J* = 4.0, 8.0 Hz, 1H, H-2), 2.92 (q, *J* = 4.0, 8.0 Hz, 1H, H-4), 2.99 (s, 3H, OMe), 3.05 (q, *J* = 8.0, 12.0 Hz, 6H, Et<sub>3</sub>N), 3.28–3.31 (m, 1H, OCH<sub>2</sub>), 3.64 (m, 1H, H-5), 3.76–3.83 (m, 2H, H-3, OCH<sub>2</sub>), 7.16–7.30 (m, 20H, aromatic), 7.40–7.42 (m, 5H, aromatic), 7.56–7.58 (m, 5H, aromatic). <sup>13</sup>C NMR (100 MHz, CDCl<sub>3</sub>) δ 8.9 (Me, Et<sub>3</sub>N), 25.6 (C-4'), 26.1 (C-3'), 30.3 (C-2'), 36.1 (CH<sub>2</sub>CO), 45.1 (C-6), 45.4 (CH<sub>2</sub>, Et<sub>3</sub>N), 54.2 (OMe), 58.1 (C-2), 66.4 (C trityl), 70.2 (C-5), 70.3 (C trityl), 71.9 (OCH<sub>2</sub>), 73.8 (C-3), 80.7 (C-4), 97.5 (C-1), 126.3, 126.7, 126.8, 127.8, 127.9, 128.0, 128.1, 128.3, 128.8, 129.0, 129.1, 146.2, 147.0, 148.7, 179.1 (CO). HRMS (ESI) Calcd for  $C_{51}H_{54}N_2O_6Na$   $[M - Na]^+$ : 813.3880, found 813.3889. Calcd for  $C_{51}H_{53}N_2O_6Na_2$   $[M - H + 2Na]^+$ : 835.3699, found 835.3696. Calcd for  $C_{51}H_{52}N_2O_6Na_3$   $[M - 2H + 3Na]^+$ : 857.3519, found 857.3553.

**Procedure for the Synthesis of PNA–Aminoglucoamine Conjugates 5a and 5b.** To a solution of the protected glucosamine derivative 15 (18 mg, 20 μmol) in dry DMF (1 mL), under argon, were added 1-[3-(dimethylaminopropyl)]-3-ethylcarbodiimide hydrochloride (5.2 mg, 30 μmol) and 1-hydroxybenzotriazole (HOBt) (4.0 mg, 30 μmol). The resulting solution was stirred for 15 min, and then the protected PNA (3a or 3b) on its solid support was added under argon (PNA synthesis at 2 μmol scale). The mixture was stirred at room temperature for 1 h and filtered. The neamine PNA conjugate was then cleaved from the solid support with concomitant deprotection by treatment with TFA/anisole (1/1) for 1 h. The mixture was filtered, and then diethyl ether was added to the solution to precipitate the PNA. HPLC purification was carried out on a C<sub>18</sub>

reversed-phase column (Macherey-Nagel, 10.0 mm × 250 mm) with a Dionex Ultimate 3000 (detection at 260 and 280 nm). Elution was performed at 60 °C at a flow rate of 2 mL/min by building up the following gradients: 0.1% TFA in acetonitrile/0.1% TFA in water (10/90 v/v) for 10 min, then 0.1% TFA in acetonitrile/0.1% TFA in water/methanol (10/85/5 v/v/v) for 5a or 0.1% TFA in acetonitrile/0.1% TFA in water (10/90 to 40/60 v/v for 30 min) for 5b.

Conjugate 5a: MALDI-TOF MS *m/z* found, 4576.0088; calcd for  $C_{183}H_{239}N_{91}O_{54}$ , 4574.8753 (noncoupled and free PNA: 4286.7068). Conjugate 5b: MALDI-TOF MS *m/z* found, 5207.2808; calcd for  $C_{216}H_{272}N_{94}O_{64}$ , 5206.0919 (noncoupled free PNA: 4917.9234).

**Biological Assays. Cellular Uptake of Fluorescein Labeled PNA–Aminoglucoamine by Flow Cytometry.** CEM (T-cell lymphocytes) cells were used to evaluate the efficiency of cellular uptake of conjugate 5b. The cells were grown at 37 °C in 5% CO<sub>2</sub> environment in complete RPMI1640 medium (GIBCO, Life Technology, USA) containing 10% fetal bovine serum and 100 units each of penicillin and streptomycin. The cells growing at log phase were harvested, washed with phosphate buffered saline, and resuspended in RPMI media with 2% FBS. Cells were aliquoted in 12-well plate at 0.5 × 10<sup>6</sup> cells/mL and incubated for 30 min at 37 °C. Fluorescein labeled PNA–aminoglucoamine conjugate 5b was added to cells at varying concentrations (50 nM–1000 nM) and incubated at 37 °C. At different time points, cells were harvested, washed twice with PBS, and resuspended in 1 mL of PBS for FACScan analysis on Becton Dickinson flow cytometer. To exclude the uptake by dead cells, the scanning was done in the presence of propidium iodide (1 μg/mL). Cell Quest Pro software (Becton Dickinson) was used to acquire and analyze events detected by FL1 detector (for FITC), which excluded FL3 detector (propidium iodide). Graphs were generated using GraphPad Prism 4.0. We also used Huh7.5 cells, which are relatively larger and have more cytoplasmic space than CEM cells. Cells were incubated with 1 μM PNA–glucosamine conjugate 5b in the absence and presence of an endosome disrupting agent, chloroquine.<sup>67</sup> After 10 h of incubation, cells were washed with PBS and stained with wheat germ agglutinin conjugated with rhodamine to label the oligosaccharides component of the membrane glycoprotein (red) and with DAPI to stain the nuclear DNA (blue). Uptake of FITC labeled PNA–glucosamine 5b shows green fluorescence measured at 488 nm. The images were acquired on Nikon AIR confocal microscope.

**Preparation of <sup>32</sup>P-Labeled HIV-1 TAR RNA and HCV 3'NTR RNA Fragment.** The plasmid pEM-7 encoding the HIV-1 TAR under the control of the T7 promoter was linearized using HindIII and transcribed to generate 82 base long runoff transcript of HIV-1 TAR RNA using T7 RNA polymerase transcription kit (Roche Diagnostics). For preparing hepatitis C virus RNA fragment corresponding to 3' tail of HCV-3'NTR, we amplified this region by PCR and then transcribing the PCR product as described before.<sup>90</sup> The RNA transcript was internally labeled using α<sup>32</sup>P-CTP (3000 Ci/mmol; Perkin-Elmer Life and Analytical Sciences). The runoff transcript was purified by phenol:chloroform:isoamyl alcohol extraction followed by ethanol precipitation. The RNA was air-dried and resuspended in water pretreated with diethyl pyrocarbonate (DEPC) and finally stored at –70 °C.

**Gel Mobility Shift Assay.** The binding affinity of the PNA–aminoglucoamine for the TAR RNA was examined by gel mobility shift assay. An aliquot of <sup>32</sup>P-labeled 82 bp long TAR RNA transcript (10 nM) was incubated with varying concentrations of conjugate 5a in a binding buffer containing 50 mM Tris-HCl (pH 7.8), 60 mM KCl, and 5 mM MgCl<sub>2</sub> in a final volume of 10 μL. After incubation at room temperature for 1 h, 10 μL of gel loading dye (0.27% bromophenol blue and 20% glycerol) was added to the samples and were run (100 V) on a native 8% polyacrylamide gel using Tris-borate-EDTA buffer at room temperature for 4 h. The gel was subjected to PhosphorImager analysis (Molecular Dynamics).

**Tat-Mediated Transactivation of HIV-1 LTR.** CEM cells (0.5 × 10<sup>6</sup> cells per well in 12 well plate) were transfected with the plasmid cocktail containing pHIV-1 LTR Luc (2 μg) and pRL-SV40 (500 ng) in the presence and absence of pCMV-Tat (2 μg) using XtremeGENE 9 DNA transfection reagent (Roche). The transfection

complexes were prepared in Opti-MEM medium using 6  $\mu\text{L}$  of transfection reagent. The transfected cells were further grown in normal growth medium (RPMI medium containing 10% fetal bovine serum, 4 mM L-glutamine, 100 U of penicillin, and 100  $\mu\text{g}$  of streptomycin per mL) at 37 °C in 5% CO<sub>2</sub> environment. After 2 h, PNA-conjugates were supplemented in the medium and cells were further grown. After 24 h, cells were harvested and washed twice with PBS. The firefly and *Renilla* luciferase activities were measured using dual-luciferase reporter assay system (Dual Luciferase Assay kit). In brief, the cells were lysed using 100  $\mu\text{L}$  of passive lysis buffer on a rocking shaker for 20 min. The lysate were centrifuged at 15000 rpm for 1 min, and supernatant was collected in fresh tubes. Luciferase assay was performed by mixing 10  $\mu\text{L}$  of cell lysate in 100  $\mu\text{L}$  of luciferase assay reagent in a 96-well plate (Fluotrac). The light emission was measured using Beckman Top count luminescence counter. Firefly luciferase activities were quenched by the addition of 100  $\mu\text{L}$  of Stop and Glo reagent to measure the *Renilla* luciferase activity. Transfection efficiencies were normalized by the expression of the *Renilla* luciferase reporter gene construct cotransfected along with the experimental plasmid.

**Production and Purification of Pseudotyped HIV-1 Virions.** Pseudotyped HIV-1 virions were produced in 293T cells as described before<sup>66</sup> by cotransfection of pNL4-3.Luc.R.E with the pVSV-G retroviral vector, encoding the vesicular stomatitis virus protein G under the control of the CMV immediate-early promoter (BD Biosciences Clontech) using the calcium phosphate transfection system (Life Technologies). The transfected cells were grown in complete Dulbecco's Modified Eagle's Medium, and the culture supernatant was saved at 24, 48, and 72 h post transfection, pooled together, and analyzed for p24 antigen using the ELISA p24 antigen kit (Zaprometrix Corp.). The pseudotyped HIV-1 virions were isolated from the culture supernatant by filtration through a 0.45  $\mu\text{m}$  pore size PVDF membrane (Millipore) followed by ultracentrifugation at 70000g for 45 min. The viral pellet was resuspended in complete Dulbecco's medium and stored at -80 °C.

**Antiviral Efficacy of Conjugate 5a.** The CEM CD4<sup>+</sup> lymphocytes 12D7 (13) were grown in RPMI-1640 medium supplemented with 10% fetal calf serum, 4 mM L-glutamine at 37 °C in 5% CO<sub>2</sub> containing humidified air. Early mid log phase cells were harvested and washed with an equal volume of PBS w/o Ca<sup>2+</sup> and Mg<sup>2+</sup>. Approximately 1  $\times$  10<sup>6</sup> cells in 1 mL of RPMI-1640 medium were incubated with pseudovirions (14 ng; equiv p24) on a rocker for 2 h. The cells were centrifuged, and after washing with 1 $\times$  PBS, resuspended in fresh complete RPMI media in a 12-well plate. After 48 h post infection, an increasing amount of conjugate 5a was supplemented in the culture medium. After 76 h, the cells were harvested, washed with 1 $\times$  PBS, and lysed in 1 $\times$  passive lysis buffer (Promega). The cell lysates were centrifuged at 15000 rpm for 15 min, and an aliquot of the supernatant was assayed to determine inhibition of HIV-1 transcription by measuring reporter luciferase activity. The IC<sub>50</sub> value was calculated using CalcuSyn (Biosoft).

**Effect of Conjugate 5a on [<sup>3</sup>H]Thymidine Incorporation into Cellular DNA in CEM Cells.** Cellular proliferation of CEM cells in the presence of conjugate 5a was determined by estimating the levels of [<sup>3</sup>H] thymidine incorporated in their nuclei. Briefly, freshly split cells were grown in the absence or presence of conjugate 5a (10  $\mu\text{M}$ ) and supplemented with 10  $\mu\text{Ci}$  of [methyl-<sup>3</sup>H]thymidine/mL (83.7 Ci/mmol). The cells were harvested at 48 h, washed with PBS, and resuspended in 200  $\mu\text{L}$  of lysis buffer containing 1% NP-40 in PBS. The nucleic acids were precipitated by adding cold 10% trichloroacetic acid (TCA). Precipitates were collected on GF/C glass fiber filters (Whatman, Inc.) and washed extensively with ice-cold 10% TCA and once in 70% ethanol. Filters were dried and placed in scintillation vials, and radioactivity was counted in the scintillation counter. Cells treated with equal amounts of DMSO were kept as control. All tests were performed in triplicate.

## ■ ASSOCIATED CONTENT

### 📄 Supporting Information

General information for the synthesis, <sup>1</sup>H and <sup>13</sup>C NMR spectra of the glucosamine derivatives and HPLC profiles of the conjugates 5a and 5b. This material is available free of charge via the Internet at <http://pubs.acs.org>.

## ■ AUTHOR INFORMATION

### Corresponding Author

\*For V.N.P.: phone, 973-972-0660; fax, 973-972-8657/5594; E-mail, [pandey@umdnj.edu](mailto:pandey@umdnj.edu). For J.-L.D.: phone, +33 4 76 63 53 17; fax, +33 4 76 63 52 98; E-mail, [Jean-Luc.Decout@ujf-grenoble.fr](mailto:Jean-Luc.Decout@ujf-grenoble.fr).

### Present Address

<sup>§</sup>Université de Poitiers/CNRS, UMR 728S, Institut de Chimie des Milieux et Matériaux de Poitiers, 4 rue Michel Brunet, 86022 Poitiers, France.

### Notes

The authors declare no competing financial interest.

## ■ ACKNOWLEDGMENTS

This work was supported by the Indo–French Centre for the Promotion of Advanced Research (IFCPAR, Project no. 3405-1, J.-L. D.) and by a grant from the NIAID/NIH (AI42520) to V.N.P.

## ■ ABBREVIATIONS USED

CPP, cell-penetrating peptides; DAPI, 4',6-diamidino-2-phenylindole; FACS, fluorescence activated cell sorter; FITC, fluorescein isothiocyanate; ODN, oligo-2'-deoxyribonucleotides; PNA, peptide (polyamide) nucleic acid; TAR, trans-activation responsive region; Tat, trans-activator of transcription

## ■ REFERENCES

- (1) Davies, J.; Gorini, L.; Davis, B. D. Misreading of RNA codewords induced by aminoglycoside antibiotics. *Mol. Pharmacol.* **1965**, *1*, 93–106.
- (2) Moazed, D.; Noller, H. F. Interaction of antibiotics with functional sites in 16S ribosomal RNA. *Nature* **1987**, *327*, 389–394.
- (3) Francois, B.; Russell, R. J. M.; Murray, J. B.; Aboul-ela, F.; Masquida, B.; Vicens, Q.; Westhof, E. Crystal structures of complexes between aminoglycosides and decoding site oligonucleotides: role of the number of rings and positive charges in the specific binding leading to miscoding. *Nucleic Acids Res.* **2005**, *33*, 5677–5690.
- (4) Recht, M. I.; Fourmy, D.; Blanchard, S. C.; Dahlquist, K. D.; Puglisi, J. D. RNA sequence determinants for aminoglycoside binding to an A-site rRNA model oligonucleotide. *J. Mol. Biol.* **1996**, *261*, 421–436.
- (5) Purohit, P.; Stern, S. Interaction of a small RNA with antibiotic and RNA ligands of the 30S subunit. *Nature* **1994**, *370*, 659–662.
- (6) Von Ahsen, U.; Noller, H. F. Footprinting the sites of interaction of antibiotics with catalytic group I intron RNA. *Science* **1993**, *260*, 1500–1503.
- (7) Von Ahsen, U.; Davies, J.; Schroeder, R. Antibiotic inhibition of group I ribozyme function. *Nature* **1991**, *353*, 368–370.
- (8) Herman, T. Drugs targeting the ribosome. *Curr. Opin. Struct. Biol.* **2005**, *15*, 355–366.
- (9) Hoch, I.; Berens, C.; Westhof, E.; Schroeder, R. Antibiotic inhibition of RNA catalysis: Neomycin B binds to the catalytic core of the td group I intron displacing essential metal ions. *J. Mol. Biol.* **1998**, *282*, 557–569.

- (10) Mikkelsen, N. E.; Brannval, M.; Virtanen, A.; Kirsebom, L. A. Inhibition of RNase P RNA cleavage by aminoglycosides. *Proc. Natl. Acad. Sci. U.S.A.* **1999**, *96*, 6155–6160.
- (11) Earnshaw, D. J.; Gait, M. J. Hairpin ribozyme cleavage catalyzed by aminoglycoside antibiotics and the polyamine spermine in the absence of metal ions. *Nucl. Acid Res.* **1998**, *26*, 5551–5561.
- (12) Tor, Y.; Hermann, T.; Westhof, E. Deciphering RNA recognition: aminoglycoside binding to the hammerhead ribozyme. *Chem. Biol.* **1998**, *5*, 277–283.
- (13) Stage, T. K.; Hertel, K. J.; Uhlenbeck, O. C. Inhibition of the hammerhead ribozyme by neomycin. *RNA* **1995**, *1*, 95–101.
- (14) Cloudest-d'Orval, B.; Stage, T. K.; Uhlenbeck, O. C. Neomycin inhibition of the hammerhead ribozyme involves ionic interactions. *Biochemistry* **1995**, *34*, 11186–11190.
- (15) Chia, J. S.; Wu, H. L.; Wang, H. W.; Chen, D. S.; Chen, P. J. Inhibition of hepatitis delta virus genomic ribozyme self-cleavage by aminoglycosides. *J. Biomed. Sci.* **1997**, *4*, 208–216.
- (16) Tok, J. B. H.; Cho, J.; Rando, R. R. Aminoglycoside antibiotics are able to specifically bind the 50-untranslated region of thymidylate synthase messenger RNA. *Biochemistry* **1999**, *38*, 199–206.
- (17) Mei, H.-Y.; Galan, A. A.; Halim, N. S.; Mack, D. P.; Moreland, D. W.; Sanders, K. B.; Truong, H. N.; Czarnik, A. W. Inhibition of an HIV-1 Tat-derived peptide binding to TAR RNA by aminoglycoside antibiotics. *Bioorg. Med. Chem. Lett.* **1995**, *5*, 2755–2760.
- (18) Zapp, M. L.; Stern, S.; Green, M. R. Small molecules that selectively block RNA binding of HIV-1 protein inhibit rev function and viral production. *Cell* **1993**, *74*, 969–978.
- (19) Tam, V. K.; Kwong, D.; Tor, Y. Fluorescent HIV-1 dimerization initiation site: design, properties, and use for ligand discovery. *J. Am. Chem. Soc.* **2007**, *129*, 3257–3266.
- (20) Ennifar, E.; Paillart, J.-C.; Bodlener, A.; Walter, P.; Weibel, A.-M.; Aubertin, A.-M.; Pale, P.; Dumas, P.; Marquet, R. Targeting the dimerization initiation site of HIV-1 RNA with aminoglycosides: from crystal to cell. *Nucleic Acids Res.* **2006**, *34*, 2328–2339.
- (21) Hermann, T. Aminoglycoside antibiotics: old drugs and new therapeutic approaches. *Cell. Mol. Life Sci.* **2007**, *64*, 1841–1852.
- (22) Carvalho, I. New insights into aminoglycoside antibiotics and derivatives. *Curr. Med. Chem.* **2007**, *14*, 1101–1119.
- (23) Zhou, J.; Wang, G.; Zhang, L.-H.; Ye, X.-S. Modifications of aminoglycoside antibiotics targeting RNA. *Med. Res. Rev.* **2007**, *3*, 279–316.
- (24) Houghton, J. L.; Green, K. D.; Chen, W.; Garneau-Tsodikova, S. The future of aminoglycosides: the end or renaissance? *ChemBioChem* **2010**, *11*, 880–902.
- (25) Dozzo, P.; Moser, H. E. New aminoglycoside antibiotics. *Expert Opin. Ther. Pat.* **2010**, *20*, 1321–1341.
- (26) Hanessian, S.; Szychowski, J.; Adhikari, S. S.; Vasquez, G.; Kandasamy, P.; Swayze, E. E.; Migawa, M. T.; Ranken, R.; Francois, B.; Wirmer-Bartoschek, J.; Kondo, J.; Westhof, E. Structure-based design, synthesis, and A-site rRNA cocrystal complexes of functionally novel aminoglycoside antibiotics: C2' ether analogues of paromomycin. *J. Med. Chem.* **2007**, *50*, 2352–2369.
- (27) Zhang, J.; Chiang, F.-I.; Takemoto, J. Y.; Bensaci, M.; Litke, A.; Czyryca, P. G.; Chang, C.-W. T. J. Surprising alteration of antibacterial activity of 5"-modified neomycin against resistant bacteria. *J. Med. Chem.* **2008**, *51*, 7563–7573.
- (28) Bera, S.; Zhanel, G. G.; Schweizer, F. Antibacterial activities of aminoglycoside antibiotics-derived cationic amphiphiles. Polyol-modified neomycin B-, kanamycin A-, amikacin- and neamine-based amphiphiles with potent broad-spectrum antibacterial activity. *J. Med. Chem.* **2010**, *53*, 3626–3631.
- (29) Bera, S.; Zhanel, G. G.; Schweizer, F. Design, synthesis and antibacterial activities of neomycin–lipid conjugates: polycationic lipids with potent Gram-positive activity. *J. Med. Chem.* **2008**, *51*, 6160–6164.
- (30) Hanessian, S.; Pachamuthu, K.; Szychowski, J.; Giguère, A.; Swayze, E. E.; Migawa, M. T.; François, B.; Kondo, J.; Westhof, E. Structure-based design, synthesis and A-site rRNA co-crystal complexes of novel amphiphilic aminoglycoside antibiotics with new binding modes: a synergistic hydrophobic effect against resistant bacteria. *Bioorg. Med. Chem. Lett.* **2010**, *20*, 7097–7101.
- (31) Bera, S.; Zhanel, G. G.; Schweizer, F. Synthesis and antibacterial activity of amphiphilic lysine-ligated neomycin B conjugates. *Carbohydr. Res.* **2011**, *346*, 560–568.
- (32) Szychowski, J.; Kondo, J.; Zahr, O.; Auclair, K.; Westhof, E.; Hanessian, S.; Keillor, J. W. Inhibition of Aminoglycoside-Deactivating Enzymes APH(3')-IIIa and AAC(6')-II by Amphiphilic Paromomycin O2'-Ether Analogues. *ChemMedChem* **2011**, *6*, 1961–1966.
- (33) Baussanne, I.; Bussière, A.; Halder, S.; Ganem-Elbaz, C.; Ouberaï, M.; Riou, M.; Paris, J.-M.; Ennifar, E.; Mingeot-Leclercq, M.-P.; Décout, J.-L. Synthesis and antimicrobial evaluation of amphiphilic neamine derivatives. *J. Med. Chem.* **2010**, *53*, 119–127.
- (34) Ouberaï, M.; El Garch, F.; Bussière, A.; Riou, M.; Alsteens, D.; Lins, L.; Baussanne, I.; Dufrene, Y. F.; Brasseur, R.; Décout, J.-L.; Mingeot-Leclercq, M.-P. The *Pseudomonas aeruginosa* membranes: a target for a new amphiphilic aminoglycoside derivative? *Biochem. Biophys. Acta, Biomembr.* **2011**, *1808*, 1716–1727.
- (35) Sainlos, M.; Hauchecorne, M.; Oudrhiri, N.; Zertal-Zidani, S.; Aissaoui, A.; Vigneron, J. P.; Lehn, J. M.; Lehn, P. Kanamycin A-derived cationic lipids as vectors for gene transfection. *ChemBioChem* **2005**, *6*, 1023–1033.
- (36) Le Gall, T.; Baussanne, I.; Halder, S.; Carmoy, N.; Montier, T.; Lehn, P.; Décout, J.-L. Synthesis and transfection properties of a series of lipidic neamine derivatives. *Bioconjugate Chem.* **2009**, *20*, 2032–2046.
- (37) Desigaux, L.; Sainlos, M.; Lambert, O.; Chèvre, R.; Letrou-Bonneval, E.; Vigneron, J. P.; Lehn, P.; Lehn, J. M.; Pitard, B. Self-assembled lamellar complexes formed by lipidic aminoglycoside derivatives and siRNA promote efficient RNA interference. *Proc. Natl. Acad. Sci. U.S.A.* **2007**, *104*, 16534–16539.
- (38) Zamecnik, P. C.; Stephenson, M. L. Inhibition of Rous sarcoma virus replication and cell transformation by a specific oligodeoxynucleotide. *Proc. Natl. Acad. Sci. U.S.A.* **1978**, *75*, 280–284.
- (39) Stephenson, M. L.; Zamecnik, P. C. Inhibition of Rous sarcoma viral RNA translation by a specific oligodeoxyribonucleotide. *Proc. Natl. Acad. Sci. U.S.A.* **1978**, *75*, 285–288.
- (40) Arya, D. P.; Coffee, R. L., Jr. DNA triple helix stabilization by aminoglycoside antibiotics. *Bioorg. Med. Chem. Lett.* **2000**, *10*, 1897–1899.
- (41) Arya, D. P.; Xue, L.; Tennant, P. Combining the best in triplex recognition: synthesis and nucleic acid binding of a BQQ–neomycin conjugate. *J. Am. Chem. Soc.* **2003**, *125*, 8070–8071.
- (42) Arya, D. P.; Coffee, R. L., Jr.; Charles, I. Neomycin induced hybrid triplex formation. *J. Am. Chem. Soc.* **2001**, *123*, 11093–11094.
- (43) Napoli, S.; Carbone, G. M.; Catapano, C.; Shaw, N.; Arya, D. P. Neomycin improves cationic lipid-mediated transfection of DNA in human cells. *Bioorg. Med. Chem. Lett.* **2005**, *15*, 3467–3469.
- (44) Kaul, M.; Barbieri, C. M.; Kerrigan, J. E.; Pilch, D. S. Coupling of drug protonation to the specific binding of aminoglycosides to the A site of 16 S rRNA: elucidation of the number of drug amino groups involved and their identities. *J. Mol. Biol.* **2003**, *326*, 1373–1387.
- (45) Kirk, S. R.; Tor, Y. Hydrolysis of an RNA dinucleoside monophosphate by neomycin B. *Chem. Commun.* **1998**, 147–148.
- (46) Belousoff, M. J.; Graham, B.; Spiccia, L.; Tor, Y. Cleavage of RNA oligonucleotides by aminoglycosides. *Org. Biomol. Chem.* **2009**, *7*, 30–33.
- (47) Irudayasamy, C.; Xi, H.; Arya, D. P. Sequence specific targeting of RNA with an oligonucleotide–neomycin conjugate. *Bioconjugate Chem.* **2007**, *18*, 160–169.
- (48) Ketomäki, K.; Virta, P. Synthesis of aminoglycoside conjugates of 2'-O-methyl oligoribonucleotides. *Bioconjugate Chem.* **2008**, *19*, 766–777.
- (49) Kiviniemi, A.; Virta, P.; Lönnberg, H. Utilization of intrachain 4'-C-azidomethylthymidine for preparation of oligodeoxyribonucleotide conjugates by click chemistry in solution and on a solid support. *Bioconjugate Chem.* **2008**, *19*, 1726–1734.

- (50) Kiviniemi, A.; Virta, P.; Lönnberg, H. Solid supported synthesis and click conjugation of 4'-C-alkyne functionalized oligodeoxyribonucleotides. *Bioconjugate Chem.* **2010**, *21*, 1890–1901.
- (51) Kiviniemi, A.; Virta, P. Synthesis of aminoglycoside-3'-conjugates of 2'-O-methyl oligoribonucleotides and their invasion to a 19F labeled HIV-1 TAR model. *Bioconjugate Chem.* **2011**, *22*, 1559–1566.
- (52) Mei, H.; Xing, L.; Cai, L.; Hong-Wei, J.; Zhao, P.; Yang, Z.-J.; Zhang, L.-R.; Zhang, L.-H. Studies on the synthesis of neamine-dinucleosides and neamine-PNA conjugates and their interaction with RNA. *Bioorg. Med. Chem. Lett.* **2008**, *18*, 5355–5358.
- (53) Nielsen, P. E.; Egholm, M.; Berg, R. H.; Buchardt, O. Sequence-selective recognition of DNA by strand displacement with a thymine-substituted polyamide. *Science* **1991**, *254*, 1497–1500.
- (54) Hanvey, J. C.; Pepper, N. J.; Bisi, J. E.; Thomson, S. A.; Cadilla, R.; Josey, J. A.; Ricca, D. J.; Hassman, C. F.; Bonham, M. A.; Au, K. G.; Carter, S. G.; Bruckenstein, D. A.; Boyd, A. L.; Noble, S. A.; Babiss, L. E. Antisense and antigenic properties of peptide nucleic acids. *Science* **1992**, *258*, 1481–1485.
- (55) Hyrup, B.; Nielsen, P. E. Peptide nucleic acids (PNA): synthesis, properties and potential applications. *Bioorg. Med. Chem.* **1996**, *4*, 5–23.
- (56) Uhlmann, E.; Peyman, A.; Breipohl, G.; Will, D. W. PNA: Synthetic Polyamide Nucleic Acids with unusual binding properties. *Angew. Chem., Int. Ed.* **1998**, *37*, 2796–2823.
- (57) Demidov, V. V.; Potaman, V. N.; Frank-Kamenetskii, M. D.; Egholm, M.; Buchard, O.; Sönnichsen, S. H.; Nielsen, P. E. Stability of peptide nucleic acids in human serum and cellular extracts. *Biochem. Pharmacol.* **1994**, *48*, 1310–1313.
- (58) Koppelhus, U.; Nielsen, P. E. Cellular delivery of peptide nucleic acid (PNA). *Adv. Drug Delivery Rev.* **2003**, *55*, 267–280.
- (59) Shiraishi, T.; Nielsen, P. E. Photochemically enhanced cellular delivery of cell penetrating peptide-PNA conjugates. *FEBS Lett.* **2006**, *580*, 1451–1456.
- (60) Pandey, V. N.; Upadhyay, A.; Chaubey, B. Prospects for antisense peptide nucleic acid (PNA) therapies for HIV. *Expert Opin. Biol. Ther.* **2009**, *9*, 975–989.
- (61) Nielsen, P. E. Gene targeting and expression modulation by peptide nucleic acids (PNA). *Curr. Pharm. Des.* **2010**, *16*, 3118–3123.
- (62) Wagstaff, K. M.; Jans, D. A. Protein transduction: cell penetrating peptides and their therapeutic applications. *Curr. Med. Chem.* **2006**, *13*, 1371–1387.
- (63) Abes, S.; Ivanova, G. D.; Abes, R.; Arzumano, A. A.; Williams, D.; Owen, D.; Lebleu, B.; Gait, M. J. Peptide-based delivery of steric-block PNA oligonucleotides. *Methods Mol. Biol.* **2009**, *480*, 85–99.
- (64) Futaki, S. Membrane permeable peptide vectors: chemistry and functional design for the therapeutic applications. *Adv. Drug Delivery Rev.* **2008**, *60*, 447–447.
- (65) Gait, M. J. Peptide-mediated cellular delivery of antisense oligonucleotides and their analogues. *Cell. Mol. Life Sci.* **2003**, *60*, 844–853.
- (66) Mehiri, M.; Uper, G.; Tripathi, S.; Di Giorgio, A.; Condom, R.; Pandey, V. N.; Patino, N. An efficient biodelivery system for antisense polyamide nucleic acid (PNA). *Oligonucleotides* **2008**, *18*, 245–256.
- (67) Turner, J. H.; Ivanova, G. D.; Verbeure, B.; Williams, D.; Arzumano, A. A.; Abes, S.; Lebleu, B.; Gait, M. J. Cell-penetrating peptide conjugates of peptide nucleic acids (PNA) as inhibitors of HIV-1 Tat-dependent trans-activation in cells. *Nucleic Acids Res.* **2005**, *33*, 6837–6849.
- (68) Chaubey, B.; Tripathi, S.; Ganguly, S.; Harris, D.; Casale, R. A.; Pandey, V. N. A PNA-transportan conjugate targeted to the TAR region of the HIV-1 genome exhibits both antiviral and virucidal properties. *Virology* **2005**, *331*, 418–428.
- (69) Tripathi, S.; Chaubey, B.; Ganguly, S.; Harris, D.; Casale, R. A.; Pandey, V. N. Anti-HIV-1 activity of anti-TAR polyamide nucleic acid conjugated with various membrane transducing peptides. *Nucleic Acids Res.* **2005**, *33*, 4345–56.
- (70) Tripathi, S.; Chaubey, B.; Barton, B. E.; Pandey, V. N. Anti HIV-1 virucidal activity of polyamide nucleic acid-membrane transducing peptide conjugates targeted to primer binding site of HIV-1 genome. *Virology* **2007**, *363*, 91–103.
- (71) El-Sayed, A.; Futaki, S.; Harashima, H. Delivery of macromolecules using arginine-rich cell-penetrating peptides: ways to overcome endosomal entrapment. *AAPS J.* **2009**, *11*, 13–22.
- (72) Charles, I.; Arya, D. P. Synthesis of neomycin-DNA/peptide nucleic acid conjugates. *J. Carbohydr. Chem.* **2005**, *24*, 145–160.
- (73) Soonsil, H.; Hyun, L. K.; Jaehoon, Y. A strategy for the design of selective RNA binding agents. Preparation and RRE RNA binding affinities of a neomycin-peptide nucleic acid heteroconjugate library. *Bioorg. Med. Chem. Lett.* **2006**, *16*, 4757–4759.
- (74) Alguacil, J.; Defaus, S.; Claudio, A.; Trapote, A.; Masides, M.; Robles, J. A straightforward preparation of aminoglycoside-dinucleotide and -diPNA conjugates via Click ligation assisted by microwaves. *Eur. J. Org. Chem.* **2010**, *20*, 3102–3109.
- (75) Riguet, E.; Tripathi, S.; Chaubey, B.; Désiré, J.; Pandey, V. N.; Décout, J.-L. A Peptide nucleic acid-neamine conjugate that targets and cleaves HIV-1 TAR RNA inhibits viral replication. *J. Med. Chem.* **2004**, *47*, 4806–4809.
- (76) Chaubey, B.; Tripathi, S.; Désiré, J.; Baussanne, I.; Décout, J.-L.; Pandey, V. N. Mechanism of RNA cleavage catalyzed by sequence specific polyamide nucleic acid-neamine conjugate. *Oligonucleotides* **2007**, *17*, 302–313.
- (77) Lai, W.-F.; Lin, M. C.-M. Nucleic acid delivery with chitosan and its derivatives. *J. Controlled Release* **2009**, *134*, 158–168.
- (78) Watanabe, K.; Kashige, N.; Nakashima, Y.; Hayashida, M.; Sumoto, K. DNA strand scission by D-glucosamine and its phosphates in plasmid pBR322. *Agric. Biol. Chem.* **1986**, *50*, 1459–65.
- (79) Watanabe, K.; Kashige, N.; Kojima, M.; Nakashima, Y. Specificity of nucleotide sequence in DNA cleavage induced by D-glucosamine and D-glucosamine-6-phosphate in the presence of copper(2+). *Agric. Biol. Chem.* **1990**, *54*, 519–525.
- (80) Kashige, N.; Kojima, M.; Nakashima, Y.; Watanabe, K.; Tachifuji, A. Function of cupric ion in the breakage of pBR322 ccc-DNA by D-glucosamine. *Agric. Biol. Chem.* **1990**, *54*, 677–684.
- (81) Kashige, N.; Kojima, M.; Watanabe, K. Correlation between DNA-breaking activity of aminosugars and the amounts of active oxygen molecules generated in their aqueous solutions. *Agric. Biol. Chem.* **1991**, *55*, 1497–1505.
- (82) Kashige, N.; Yamaguchi, T.; Ohtakara, A.; Mitsutomi, M.; Brimacombe, J. S.; Miake, F.; Watanabe, K. Structure-activity relationships in the induction of single-strand breakage in plasmid pBR322 DNA by amino sugars and derivatives. *Carbohydr. Res.* **1994**, *257*, 285–291.
- (83) Vourloumis, D.; Winters, G. C.; Takahashi, M.; Simonsen, K. B.; Ayida, B. K.; Shandrick, S.; Zhao, Q.; Hermann, T. Novel acyclic deoxystreptomycin mimetics targeting the ribosomal decoding site. *ChemBioChem* **2003**, *4*, 879–885.
- (84) Crich, D.; Vinod, A. U. Oxazolidinone protection of N-acetylglucosamine confers high reactivity on the 4-hydroxy group in glycosylation. *Org. Lett.* **2003**, *5*, 1297–1300.
- (85) Takahashi, S.; Inoue, H.; Kuzuhara, H. Preparation of a highly functionalized cyclopentane derivative suitable for the synthesis of allosamidin analogues. *J. Carbohydr. Chem.* **1995**, *14*, 273–285.
- (86) Tomoda, H.; Kishimoto, Y.; Lee, Y. C. Temperature effect on endocytosis and exocytosis by rabbit alveolar macrophages. *J. Biol. Chem.* **1989**, *264*, 15445–15450.
- (87) Shiraishi, T.; Nielsen, P. E. Enhanced delivery of cell-penetrating peptide-peptide nucleic acid conjugates by endosomal disruption. *Nature Protoc.* **2006**, *1*, 1–3.
- (88) Jeang, K. T.; Xiao, H.; Rich, E. A. Multifaceted activities of the HIV-1 transactivator of transcription Tat. *J. Biol. Chem.* **1999**, *274*, 28837–28840.
- (89) Karn, J. Tackling Tat. *J. Mol. Biol.* **1999**, *293*, 235–254.
- (90) Zhang, Z.; Harris, D.; Pandey, V. N. The FUSE binding protein is a cellular factor required for efficient replication of hepatitis C virus. *J. Virol.* **2008**, *82*, 5761–5773.